



ESCUELA TÉCNICA SUPERIOR DE INGENIERÍA (ICAI)  
INGENIERO INDUSTRIAL

# **The engineering design of a formula SAE racing car**

Autor: Francisco J. Suárez Suárez  
Director: Ronald Mathews

Madrid  
Junio y 2018

Francisco J.  
Suárez  
Suárez

**The Engineering Design of a Formula SAE racing car**



**AUTHORIZATION FOR DIGITALIZATION, STORAGE AND DISSEMINATION IN THE NETWORK OF END-OF-DEGREE PROJECTS, MASTER PROJECTS, DISSERTATIONS OR BACHILLERATO REPORTS**

***1. Declaration of authorship and accreditation thereof.***

The author Mr. /Ms. Francisco Javier Suarez Suarez

**HEREBY DECLARES** that he/she owns the intellectual property rights regarding the piece of work: The Engineering Design of a FSAE Racing Car that this is an original piece of work, and that he/she holds the status of author, in the sense granted by the Intellectual Property Law.

***2. Subject matter and purpose of this assignment.***

With the aim of disseminating the aforementioned piece of work as widely as possible using the University's Institutional Repository the author hereby **GRANTS** Comillas Pontifical University, on a royalty-free and non-exclusive basis, for the maximum legal term and with universal scope, the digitization, archiving, reproduction, distribution and public communication rights, including the right to make it electronically available, as described in the Intellectual Property Law. Transformation rights are assigned solely for the purposes described in a) of the following section.

***3. Transfer and access terms***

Without prejudice to the ownership of the work, which remains with its author, the transfer of rights covered by this license enables:

- a) Transform it in order to adapt it to any technology suitable for sharing it online, as well as including metadata to register the piece of work and include "watermarks" or any other security or protection system.
- b) Reproduce it in any digital medium in order to be included on an electronic database, including the right to reproduce and store the work on servers for the purposes of guaranteeing its security, maintaining it and preserving its format.
- c) Communicate it, by default, by means of an institutional open archive, which has open and cost-free online access.
- d) Any other way of access (restricted, embargoed, closed) shall be explicitly requested and requires that good cause be demonstrated.
- e) Assign these pieces of work a Creative Commons license by default.
- f) Assign these pieces of work a HANDLE (*persistent URL*), by default.

***4. Copyright.***

The author, as the owner of a piece of work, has the right to:

- a) Have his/her name clearly identified by the University as the author
- b) Communicate and publish the work in the version assigned and in other subsequent versions using any medium.
- c) Request that the work be withdrawn from the repository for just cause.
- d) Receive reliable communication of any claims third parties may make in relation to the work and, in particular, any claims relating to its intellectual property rights.

***5. Duties of the author.***

The author agrees to:

- a) Guarantee that the commitment undertaken by means of this official document does not infringe any third party rights, regardless of whether they relate to industrial or intellectual property or any other type.

- b) Guarantee that the content of the work does not infringe any third party honor, privacy or image rights.
- c) Take responsibility for all claims and liability, including compensation for any damages, which may be brought against the University by third parties who believe that their rights and interests have been infringed by the assignment.
- d) Take responsibility in the event that the institutions are found guilty of a rights infringement regarding the work subject to assignment.

**6. Institutional Repository purposes and functioning.**

The work shall be made available to the users so that they may use it in a fair and respectful way with regards to the copyright, according to the allowances given in the relevant legislation, and for study or research purposes, or any other legal use. With this aim in mind, the University undertakes the following duties and reserves the following powers:

- a) The University shall inform the archive users of the permitted uses; however, it shall not guarantee or take any responsibility for any other subsequent ways the work may be used by users, which are non-compliant with the legislation in force. Any subsequent use, beyond private copying, shall require the source to be cited and authorship to be recognized, as well as the guarantee not to use it to gain commercial profit or carry out any derivative works.
- b) The University shall not review the content of the works, which shall at all times fall under the exclusive responsibility of the author and it shall not be obligated to take part in lawsuits on behalf of the author in the event of any infringement of intellectual property rights deriving from storing and archiving the works. The author hereby waives any claim against the University due to any way the users may use the works that is not in keeping with the legislation in force.
- c) The University shall adopt the necessary measures to safeguard the work in the future.
- d) The University reserves the right to withdraw the work, after notifying the author, in sufficiently justified cases, or in the event of third party claims.

Madrid, on May..... of 2018.....

**HEREBY ACCEPTS**

Signed.....  .....

Reasons for requesting the restricted, closed or embargoed access to the work in the Institution's Repository

Declaro, bajo mi responsabilidad, que el Proyecto presentado con el título  
**THE ENGINEERING DESIGN OF A FORMULA SAE RACING CAR**  
en la ETS de Ingeniería - ICAI de la Universidad Pontificia Comillas en el  
curso académico **2017/2018** es de mi autoría, original e inédito y  
no ha sido presentado con anterioridad a otros efectos. El Proyecto no es  
plagio de otro, ni total ni parcialmente y la información que ha sido tomada  
de otros documentos está debidamente referenciada.

Fdo.: **Francisco Javier Suárez Suárez** Fecha: **08/ 05/2018**

Autorizada la entrega del proyecto  
EL DIRECTOR DEL PROYECTO

Fdo.: **Ronald Matthews** Fecha: **08/ 05/2018**

Handwritten signature of Ronald Matthews in black ink.



ESCUELA TÉCNICA SUPERIOR DE INGENIERÍA (ICAI)  
INGENIERO INDUSTRIAL

# **The engineering design of a formula SAE racing car**

Autor: Francisco J. Suárez Suárez  
Director: Ronald Mathews

Madrid  
Junio y 2018

Francisco J.  
Suárez  
Suárez

**The Engineering Design of a Formula SAE racing car**



# **THE ENGINEERING DESIGN OF A FORMULA SAE RACING CAR**

**Autor: Suárez Suárez, Francisco J.**

**Director: Matthews, Ronald**

**Entidad Colaboradora: Long Horn Racing Electric**

**RESUMEN DEL PROYECTO**



# 1. ABSTRACT

El objetivo de este TFM es analizar, rediseñar y mejorar diferentes subsistemas de un fórmula SAE eléctrico. Long Horn Racing Electric desarrolla un coche nuevo cada año para la FSAE competición, donde los coches son puestos a prueba en diferentes campos, como resistencia o aceleración. Para construir un coche competitivo, el chasis, la suspensión delantera y trasera del coche de año pasado van a ser analizadas y rediseñadas. Usando información obtenida de los diseños del año pasado, se van a crear y probar nuevos diseños con el objetivo de mejorar la eficiencia global del coche. Peso, aceleración, rigidez torsional y ratios de movimiento son un ejemplo de los KPI que se utilizarán para medir las mejoras

## 2. DISEÑO DEL CHASIS

### 2.1. INTRODUCCIÓN

El chasis de un coche es una estructura hecha de barras que se encarga de proteger al piloto en caso de accidente y de sostener al resto de subsistemas. Es uno de los subsistemas más importantes de un FSAE, puesto que es responsable de la mayoría del peso del monoplaza. Mejorar su diseño y eficiencia afecta directamente al manejo, la aceleración y el consumo.

### 2.2. ESTADO DEL ARTE

El chasis de 2017 fue diseñado para ser simple y robusto. El diseño fue muy influenciado por los consejos del equipo de combustión interna, siendo el diseño final muy parecido al desarrollado por ellos, pero con unas pocas modificaciones para incluir los diferentes sistemas eléctricos. El chasis estaba compuesto principalmente por tubos de 1 pulgada de diámetro y no variaba mucho. La zona del acumulador, antiguamente motor, fue reforzada y ampliada. La caja trasera fue triangulada y, en algunas partes, reforzada para sostener al motor y los palieres. Algunos de los tubos que soportan la suspensión fueron reforzados.

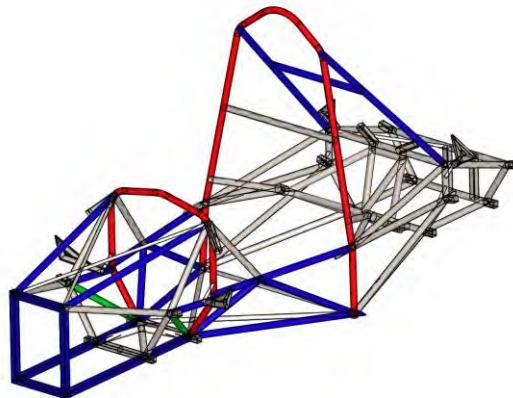


FIGURE 1: CHASIS DE 2017

El equipo nunca había realizado ningún análisis o simulación en el chasis de 2017. Ellos afirman que intentaron realizar un análisis estático sin éxito debido a problemas con la mesh.

### 2.3. ANÁLISIS DE LA RIGIDEZ TORSIONAL

Como el chasis de 2017 resistió toda la competición sin romperse, su valor de rigidez torsional va a ser usado como límite superior. Después de modificar el modelo de CAD para poder realizar FEA, el valor de rigidez torsional obtenido fue de 1900 lbf-in/deg.

El prototipo del chasis de 2018 fue modificado usando técnicas similares a las usadas para el modelo de 2017, pero si éxito. El modelo tuvo que ser reconstruido tubo a tubo y creando la mesh después de cada iteración para descubrir el problema. El modelo del chasis de 2018 refinado se muestra en Figure 2. La rigidez torsional obtenida fue de 1165 lbf-ft/deg.

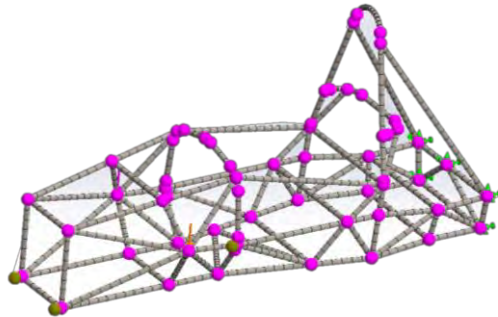


FIGURE 2: MESH DEL PROTOTIPO DE 2018

### 2.4. MEJORA DEL DISEÑO

Carroll Smith (1932–2003) fue un exitoso piloto profesional, ingeniero y autor. Escribió varios libros sobre ingeniería de competición, como Tune to Win. El ayudó al equipo de combustión interna hace años y dio a los distintos equipos de UT SAE un valor objetivo de la rigidez torsional de 1500 lbf-ft. Este valor también se obtiene buscando que el chasis sea mucho más rígido que la suspensión. Si se multiplica la rigidez torsional de la suspensión por 10 se obtiene un valor muy cercano a 1500 lbf-ft.

Diferentes modificaciones de diseño fueron probadas intentando aproximarse lo máximo posible a dicho valor a la vez que se trató de minimizar el incremento de peso. Después de más de 15 iteraciones, la rigidez torsional del chasis se aumentó en un 34% a 1556 lbf-ft incrementando el peso solo un 2.4%. En la Figure 3 se observa el chasis finalizado.



FIGURE 3: CHASIS DE 2018

### 3. DISEÑO DEL SISTEMA DE BELLCRANKS

#### 3.1. INTRODUCCIÓN

Una bellcrank es un cuerpo sólido que cambia el movimiento mediante un ángulo, rotando en un punto fijo. El sistema consiste en un pushrod, la bellcrank, el amortiguador y la barra de anti-rol. En un coche de competición, las bellcranks se encargan de transmitir la fuerza generada por el pushrod a la suspensión y a la barra de anti-rol y de definir el Instalation Ratio (IR), que se define como la cantidad de compresión que experimenta el amortiguador por unidad de movimiento de la rueda. Este ratio es de suma importancia para el manejo, puesto que mide como el coche rueda lateralmente en las curvas

#### 3.2. DISEÑO PREVIO

Las bellcranks de 2017 se muestran en la Figure 4. Estaban hechas de acero y no fueron sujeto de ningún análisis. No se hicieron cálculos del IR, y fueron diseñadas simplemente para que los componentes del sistema no interfiriesen entre sí.

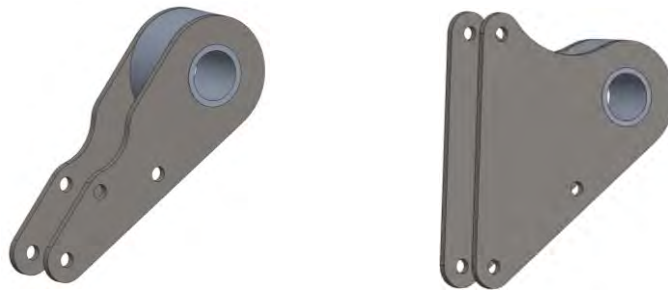
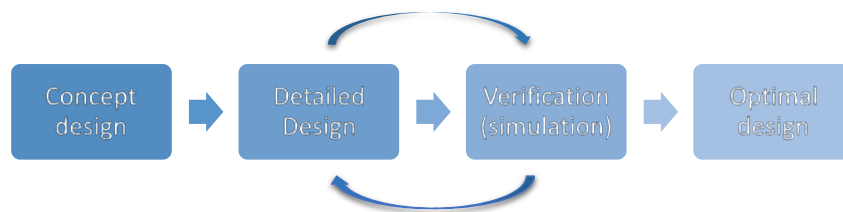


FIGURE 4: BELLCRANK DELANTERA Y TRASERA DE 2017, RESPECTIVAMENTE

#### 3.3. PROCESO DE DISEÑO

El primer paso en el proceso de diseño es determinar las frecuencias de conducción. Como la pista tiene baches, es necesario aplicar flat tuning buscando diferentes frecuencias de conducción delante y detrás. Usando estos valores y la constante de los muelles y las ruedas es posible obtener el IR deseado.

El ciclo de diseño tradicional se muestra en el siguiente gráfico:



Sin embargo, para este proceso de diseño se empleó la optimización topológica. Este proceso reduce considerablemente el tiempo de diseño y el número de iteraciones:



### 3.3.1. ESPACIO DE DISEÑO

El espacio de diseño se define como el máximo volumen que una pieza puede tener sin interferir con otros elementos. Para una bellcrank es una parte muy importante del diseño, puesto que también define el IR. Este ratio queda definido por la posición relativa de las monturas de los diferentes componentes y puesto que normalmente la compresión del muelle y el viaje de la rueda no ocurren en el mismo plano, es muy difícil de ajustar.

Para la bellcrank trasera, se usó el Dynamic Reference Sketch (DRS) para ajustar el IR. Esta herramienta de SolidWorks está compuesta por 3D sketches con relaciones geométricas y ecuaciones que permiten diseñar y verificar diferentes parámetros de la suspensión, como la variación del camber y el anti-squad. El DRS fue modificado para incorporar las bellcranks y medir el IR. Esto se muestra en la Figure 5. Para comprobar la existencia de interferencias, un assembly con todas las partes fue creado tanto para máxima compresión como extensión.

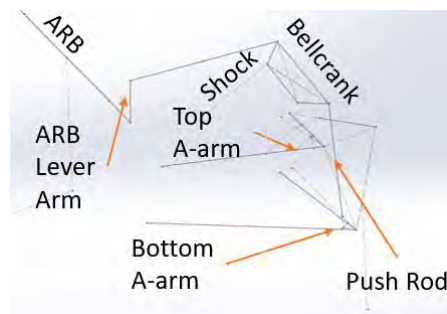


FIGURE 5: BELLCRANK SYSTEM EN EL DRS

Para la bellcrank delantera, la metodología de diseño fue mejorada. En vez de emplear el DRS, se empleó un Motion Study de SolidWorks. Esta metodología permite combinar el chequeo de interferencias con la medida del IR. El Motion Study anima el assembly de acuerdo con las mates especificadas para simular el movimiento de la suspensión por completo, lo que permite comprobar los distintos requisitos de diseño en todo el viaje de la suspensión. Figure 6 muestra el modelo de la suspensión usado y el gráfico del IR durante el viaje de la suspensión.

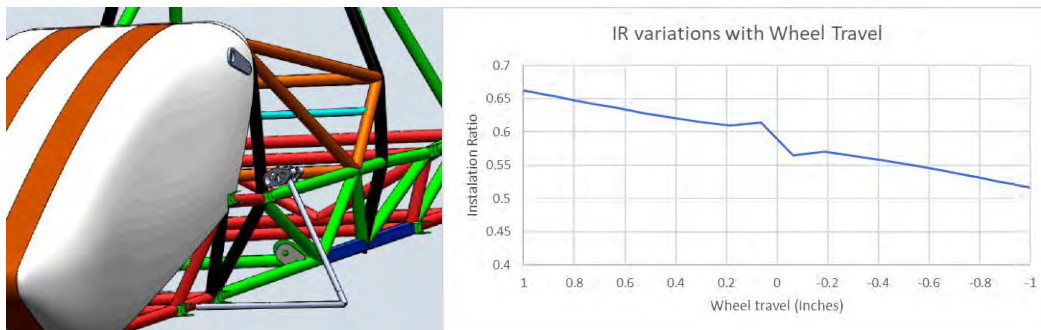


FIGURE 6: ASSEMBLY PARA EL MOTION STUDY Y EL GRÁFICO DEL IR

### 3.3.2. OPTIMIZACIÓN TOPOLÓGICA

Los programas de optimización topológica se usan para minimizar el peso de diferentes piezas quitando material del espacio de diseño que no está sujeto a una cantidad determinada de tensión o compresión de acuerdo con múltiples casos de cargas y fijaciones. SolidThinking Inspire fue el software utilizado para realizar la optimización topológica. Como aun se encuentra en fase de desarrollo, no es posible importar piezas directamente desde SolidWorks student edition. La única opción era exportar las piezas como parasolidos, lo que impide importar los sketches usados para obtener las direcciones de las fuerzas.

Como la bellcrank trasera fue diseñada con el mismo sistema de referencia que el coche para facilitar el ensamblamiento, todas las coordenadas de los vectores de fuerzas están en esa base. El problema con este sistema de referencia es que Inspire necesita un plano de simetría en el medio de la parte para que pueda ser fabricada con una máquina CNC, pero los planos de la pieza no estaban alineados con la misma. Inspire solo dejaba rotar los planos introduciendo a mano el valor del ángulo que se desea rotar, por lo que se tuvo que resolver el problema inverso de los ángulos de Euler. La bellcrank delantera fue creada con su propio sistema de referencia buscando evitar este problema, pero al hacer esto fue necesario cambiar de base todos los vectores de fuerzas puesto que habían sido calculados en la base del coche.

Las fuerzas fueron calculadas buscando el peor escenario posible en todos los casos, puesto que el programa de optimización topológica se basa en fuerzas estáticas y nuestro caso es dinámico, obteniendo así un factor de seguridad extra. La máxima fuerza del amortiguador fue calculada como la máxima compresión por el máximo recorrido del mismo y la fuerza de la barra de anti-rol usando el máximo par que transmite sin romperse. Se fijó la montura del chasis y la montura del pushrod con fisura de bisagra, ya que el pushrod aplica una fuerza igual a la suma de las otras mas la inercia, despreciada en este caso. Se eligió un factor de seguridad de 2 en cada pieza puesto que al no poder crear prototipos el factor de seguridad habitual de 1.2 era muy arriesgado para el ahorro en peso que proporcionaba.

### 3.4.FINAL DESIGN

El diseño final de ambas bellcranks se muestra en la Figure 7. La CNC fue programada usando HSM Works. Se redujo el peso un 64% y un IR constante para la bellcrank trasera y una reducción de peso del 72% y un  $\pm 7.1\%$  de variación en el IR para la bellcrank delantera.

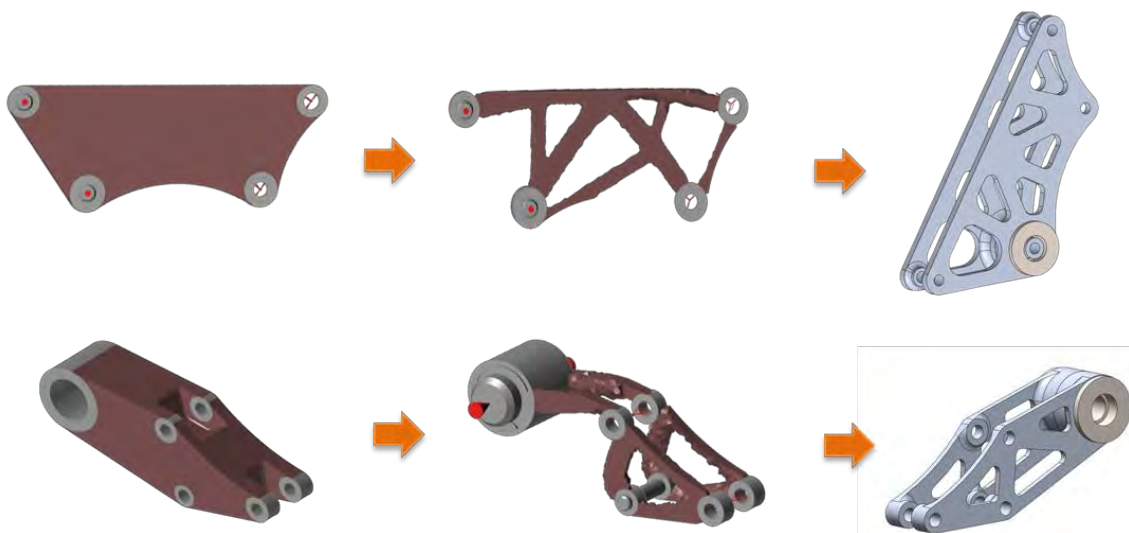


FIGURE 7: ESPACIO DE DISEÑO, OPTIMIZACIÓN TOPOLÓGICA Y MODELO FINAL

# **THE ENGINEERING DESIGN OF A FORMULA SAE RACING CAR**

**Autor: Suárez Suárez, Francisco J.**

**Director: Matthews, Ronald**

**Entidad Colaboradora: Long Horn Racing Electric**

**PROJECT SUMMARY**

# 1. ABSTRACT

The objective of this research is to analyze, redesign and improve different subsystem of a formula SAE electric single-seater car. Long Horn Racing Electric develop a new car each year for the Formula SAE competition, where the cars are tested in different fields, such as endurance or acceleration. To build a competitive car, the chassis, front and rear suspensions of last year single seater are going to be analyzed and redesigned. Using the data obtained from the last year's car, new designs are going to be tested in order to improve the overall efficiency. Weight, acceleration, torsional stiffness and motion ratios are some key performance indicators which are going to be used for measuring the improvements.

## 2. CHASSIS DESIGN

### 2.1. INTRODUCTION

A car's chassis is a structure made up of beams that is in charge of protecting the driver in the case of an accident and holding all subsystem together. It is one of the most important subsystem of a FSAE car, as it has the majority of the weight of the single seater. Improving its design and efficiency have direct effects in handling, acceleration, fuel efficiency.

### 2.2. STATE OF THE ART

The 2017 chassis was designed for simplicity and robustness is in design and manufacturing. Drawing heavily from advice from Longhorn Racing IC, the chassis is very similar to an existing internal combustion chassis, with modifications to allow for an electric drive system, accumulator, and the extra weight. The chassis is comprised of mostly 1-inch diameter tubing and deviates very little from the given tube sizes. The accumulator, previously engine, bay was enlarged and reinforced. The rear box was also triangulated and, in some parts, thickened to contain the motor and spool. Some of the front tubes supporting the suspension points were also thickened or reinforced.

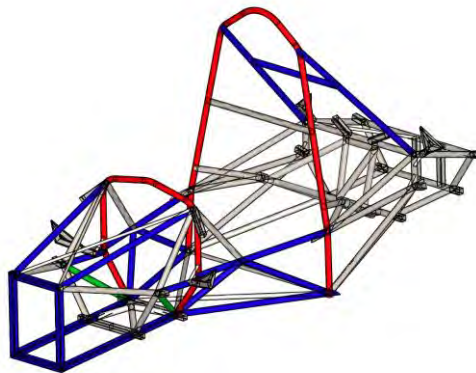


FIGURE 1: 2017 CHASSIS

The electric team has never realized any analysis on the 2017 frame. They stated that they tried to run a static analysis without success due to problems while meshing.



### 2.3. TORSIONAL STIFFNESS ANALYSIS

As the 2017 chassis resisted through all the competition, its torsional stiffness value is going to be used as an upper limit. After modifying the CAD model to make it FEA suitable, the torsional stiffness value was 1900 lbf-in/deg.

The 2018 frame prototype was modified using similar techniques as the ones used for the 2017 chassis, without success. The model was then rebuilt beam by beam and meshing after each iteration in order to discover which beams were causing problems. The 2018 FEA suitable model is shown in Figure 2. The torsional stiffness of this version was 1165 lbf-ft/deg.

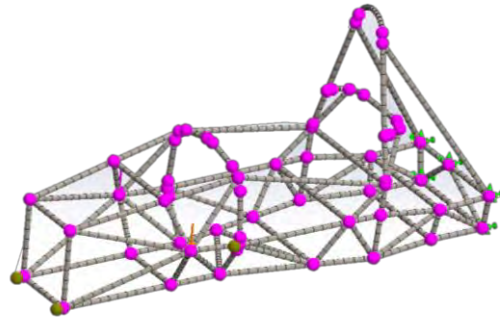


FIGURE 2: MESH OF 2018 FRAME PROTOTYPE

### 2.4. DESIGN MODIFICATIONS

Carroll Smith (1932–2003) was a successful professional race car driver, engineer, and author. He wrote several race car engineering books, such as *Tune to Win*. He helped the combustion team years ago and gave UT SAE a target value for torsional stiffness of 1500 lbf-ft. This value can also be obtained by considering that the frame has to be much more rigid than the suspension. Multiplying the suspension torsional stiffness by 10 also gives a value of 1500 lbf-ft/deg.

Different design modifications were tested trying to approach as much as possible to the target torsional stiffness while minimizing the weight increase. After more than 15 combinations, the torsional stiffness was increased a 34% to 1556 lbf-ft/deg while only increasing weight a 2.4%. Figure 3 depicts the 2018 final frame manufactured.

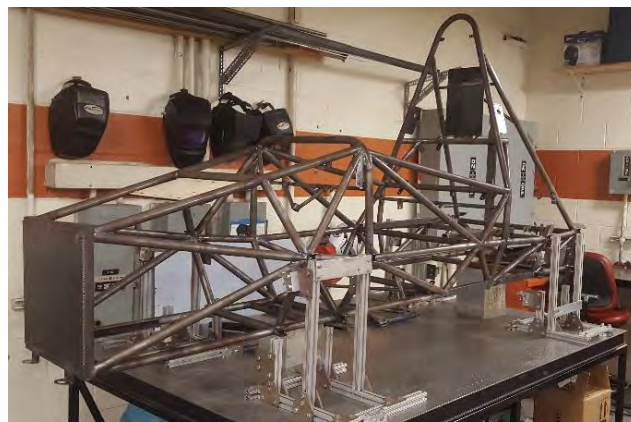


FIGURE 3: 2018 FRAME



### 3. BELLCRANK SYSTEM DESIGN

#### 3.1. INTRODUCTION

A bellcrank is a solid body which changes motion through an angle, by rotating about a point. The system consists in the pushrod, the bellcrank itself, the shock and the antiroll bar. In a race car, bellcranks are in charge of transferring the forces generated by the pushrod and the ARB to the shock absorber and defining the Installation Ratio (IR), which is defined as unit shock compression per unit wheel travel. This ratio is very important for handling, as it is a measure of how the car rolls in corners.

#### 3.2. STATE OF THE ART

2017 front and rear bellcranks are shown in Figure 4. They were made of steel and they did not have had any analysis. No Installation ratio calculations were performed in these models, they were designed for clearance and durability.

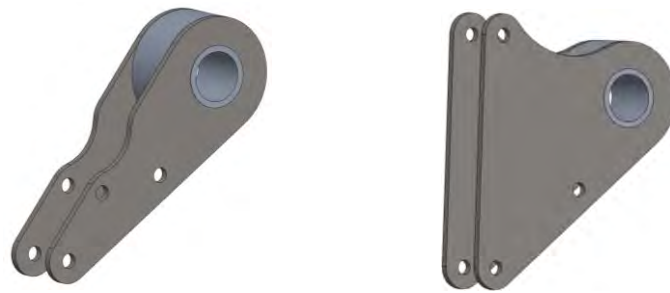
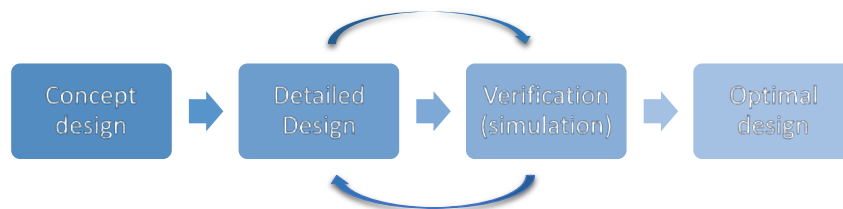


FIGURE 4: 2017 FRONT BELLCRANK AND REAR BELLCRANK, RESPECTIVELY

#### 3.3. DESIGN PROCESS

The first step in the design process is to determine the ride frequencies. As the track is bumpy, flat tuning needs to be applied, aiming for different ride frequencies in the front and rear. Using these values and the shock constants, desired installation ratios are obtained.

The traditional design cycle is depicted in the next graph:



However, for this design process, the topological optimization design approach was used. It is supposed to considerably reduce design time and the number of iterations:



### 3.3.1. DESIGN SPACE

The design space is defined as the maximum volume that a part can have without interfering with other elements. For a bellcrank it is an important part of the design process as it also defines the Installation Ratio. This ratio is defined by the relative position of the mounts of the different components and as the wheel displacement and shock compression occur in different planes, the adjustment of the ratio is not trivial.

For the Rear Bellcrank, the Dynamic Reference Sketch (DRS) was used to tune the rear IR. This SolidWorks tool is made of 3D sketches with geometrical relations and equations that allow to design and verify different suspension parameters, such as camber variations or anti-squad. The sketch was modified in order to incorporate the bellcrank system and a measure of the IR. This is shown in Figure 5. To check for clearance, assemblies with all the parts from the frame and suspension for maximum compression and maximum tension were created.

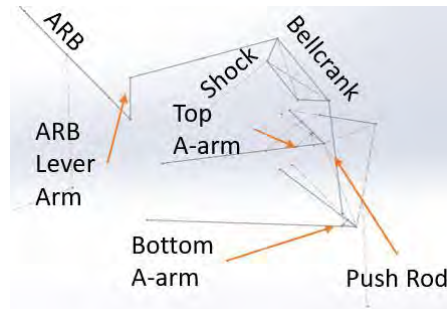


FIGURE 5: BELLCRANK SYSTEM IN THE DRS

For the Front Bellcrank, the design methodology was improved. Instead of using the DRS, a SolidWorks Motion Study was created. This methodology allowed to combine the clearance check with the measurement of the IR. The motion study animates an assembly according to its mates to simulate the suspension movements, which allows to check constraints through all wheel travel. Figure 6 depicts the suspension model used for the motion study and the IR plot generated by the Motion Study.

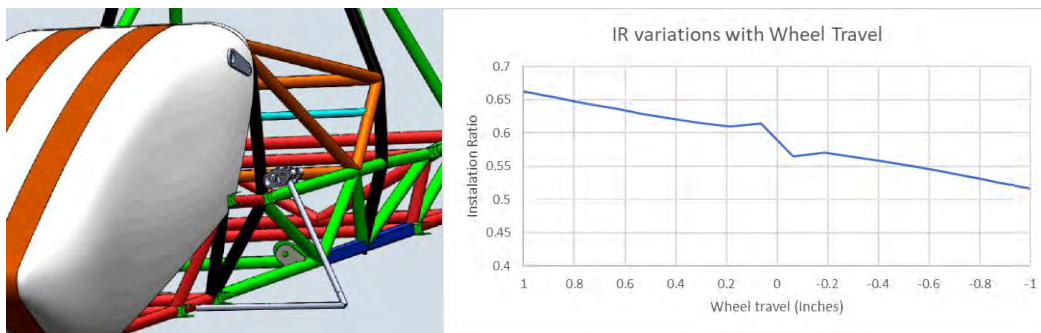


FIGURE 6: ASSEMBLY FOR MOTION STUDY AND IR PLOT

### 3.3.2. TOPOLOGICAL OPTIMIZATION

Topological optimization software are used to minimize the weight of a part by removing material of design spaces that are not under a certain amount of stress according to multiple load cases and fixtures. SolidThinking Inspire was the software used to perform the topological optimization. As it is in a development stage, it was not possible to import parts from the SolidWorks student edition. The only option was to import the part as a parasolid, which does not allow to import the sketches used to obtain the direction of the forces for the compression and tension load cases.

As the Rear Bellcrank was modeled with the same reference system as the car reference system in order to make assemblies easier, all the forces vectors coordinates were calculated with this origin as base. The problem with this base was that the software needed to have a symmetry plane in the middle of the part in order to be CNC manufacturable and the original symmetry planes were the ones of the car, not the part. The only option to modify them to match with the part plane was to insert an angle of rotation manually, which had to be obtained by solving the invers Euler's angle problem. The front bellcrank design space was created with its own reference system in order to avoid the last problem, but by doing this, all the force vectors needed to have their bases changed as the sketch used has the reference system matching with the car's one.

The forces were calculated as the worst-case scenario loads because topological optimization is based in static analysis and the parts designed are going to be under dynamic loads. The maximum shock force was obtained assuming maximum shock compression and for the anti roll bar, the torque that would cause it to fail was obtained and then transformed into a force value. The fixtures used were hinges, both un the frame and pushrod mount, as the pushrod had to apply a force equivalent to the sum the other forces plus the inertia, which can be ignored. For both parts a factor of safety of 2 was used as the budget did not allowed to create prototypes and the difference in mass from a 1.2 FOS related to a 2 was only 15%.

### 3.4.FINAL DESIGN

The final design process of both bellcranks is depicted in Figure 7. The definitive model was designed with manufacturability in mind. The CNC was programed using HSM Works. There was a 64% weight reduction and a constant IR for the RBC, and a 72% weight reduction and a  $\pm 7.1\%$  variation of the desired IR for the FBC.

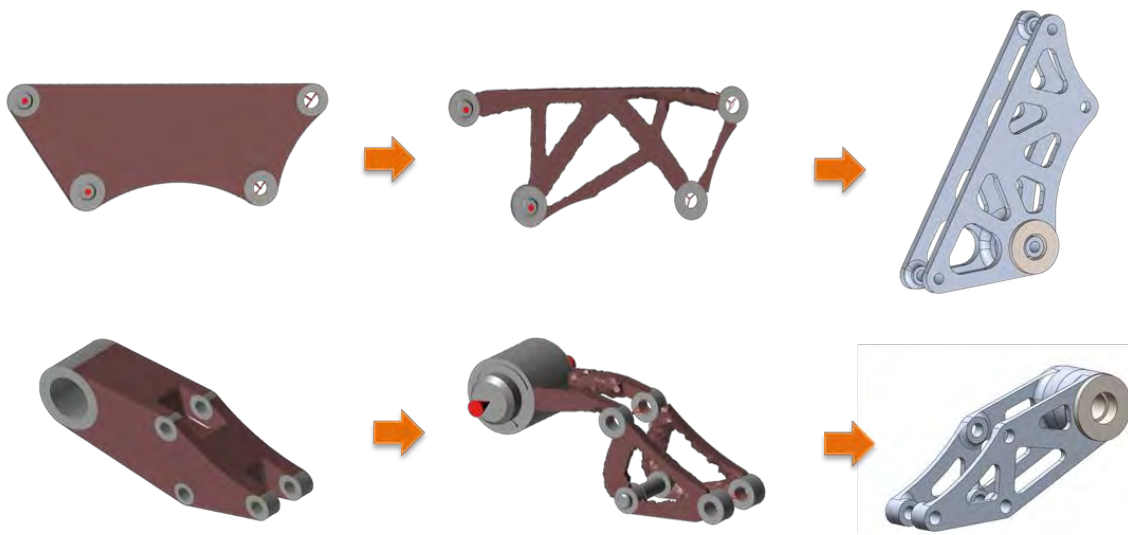


FIGURE 7: DESIGN SPACE, TOPOLOGICAL OPTIMIZATION AND DEFINITIVE MODEL FOR FBC AND RBC RESPECTIVELY

Copyright  
by  
Francisco J. Suarez Suarez  
2018

## The Engineering design of a FSAE Racing Car

APPROVED BY

SUPERVISING COMMITTEE:

---

Ronald Matthews, Supervisor

---

Jose Ignacio Linares Hurtado

**The Engineering design of a FSAE Racing Car**

by

**Francisco J. Suarez Suarez, B.S.**

**THESIS**

Presented to the Faculty of the Graduate School of

The University of Texas at Austin

in Partial Fulfillment

of the Requirements

for the Degree of

**MASTER OF SCIENCE IN INDUSTRIAL ENGINEERING**

THE UNIVERSITY OF TEXAS AT AUSTIN

June 2018

Dedicated to my friends and family.

## Acknowledgments

I wish to thank all the members of Long Horn Racing Electric. Without their work and dedication this thesis would not be possible.



# The Engineering design of a FSAE Racing Car

Francisco J. Suarez Suarez, M.S.  
The University of Texas at Austin, 2018

Supervisor: Ronald Matthews

The objective of this research is to analyze, redesign and improve different subsystem of a formula SAE electric single-seater car. Long Horn Racing Electric develop a new car each year for the Formula SAE competition, where the cars are tested in different fields, such as endurance or acceleration. To build a competitive car, the chassis, front and rear suspensions of last year single seater are going to be analyzed and redesigned. Using the data obtained from the last years car, new designs are going to be tested in order to improve the overall efficiency. Weight, acceleration, torsional stiffness and motion ratios are some key performance indicators which are going to be used for measuring the improvements.

# Table of Contents

<b>Acknowledgments</b>	<b>v</b>
<b>Abstract</b>	<b>vi</b>
<b>List of Tables</b>	<b>x</b>
<b>List of Figures</b>	<b>xi</b>
<b>Chapter 1. Introduction</b>	<b>1</b>
1.1 Chassis . . . . .	1
1.2 Suspension . . . . .	2
<b>Chapter 2. Customer information</b>	<b>4</b>
2.1 Background of need . . . . .	4
2.2 Customer Needs Statement . . . . .	5
2.3 Vehicle requirements . . . . .	6
2.4 Functional Requirements . . . . .	6
2.5 Long Horn Racing Electric working methodology . . . . .	7
<b>Chapter 3. State of the art</b>	<b>10</b>
3.1 Frame . . . . .	10
3.2 Suspension . . . . .	11
<b>Chapter 4. Frame Design</b>	<b>14</b>
4.1 Chassis . . . . .	14
4.2 Previous work . . . . .	14
4.3 Design objectives . . . . .	15
4.4 Design methodology . . . . .	18
4.5 Torsional stiffness calculation for 2017 frame . . . . .	19
4.6 Torsional stiffness calculation for 2018 frame . . . . .	23

4.6.1	Preparation of 2018 model for FEA . . . . .	23
4.6.2	Torsional stiffness accuracy . . . . .	26
4.7	Design modifications for 2018 frame . . . . .	30
<b>Chapter 5. Bellcrank Design</b>		<b>34</b>
5.1	Bellcrank system . . . . .	34
5.2	Previous work . . . . .	35
5.3	Installation ratio calculation for 2018 bellcranks . . . . .	35
5.4	Dynamic Reference Sketch . . . . .	37
5.5	Anti-roll bar (ARB) . . . . .	38
5.6	Nosecone . . . . .	39
5.7	Design objectives . . . . .	39
5.8	Design methodology . . . . .	40
5.9	Rear Bellcrank Design Process . . . . .	41
5.9.1	Design Space . . . . .	43
5.9.2	Topological optimization . . . . .	45
5.9.3	Final rear bellcrank design . . . . .	51
5.10	Front Bellcrank Design . . . . .	52
5.10.1	Motion study . . . . .	53
5.10.2	Motion study refinements . . . . .	54
5.10.3	Design space . . . . .	58
5.10.4	Topological optimization . . . . .	61
5.10.5	Front bellcrank final design . . . . .	64
<b>Chapter 6. Project schedule and budget</b>		<b>66</b>
<b>Chapter 7. Conclusions</b>		<b>69</b>
7.1	Frame . . . . .	69
7.2	Suspension . . . . .	71
7.3	Manufacturability . . . . .	73
7.4	Future works . . . . .	73
7.4.1	Frame . . . . .	73
7.4.2	Suspension . . . . .	75

<b>Appendices</b>	<b>77</b>
<b>Appendix A. Calculations and selection of frame design modifications</b>	<b>78</b>
A.1 Test 1 . . . . .	79
A.2 Test 2 . . . . .	81
A.3 Test 3 . . . . .	82
A.4 Test 4 . . . . .	84
<b>Appendix B. Rotation of SolidThinking Inspire Planes</b>	<b>86</b>
<b>Appendix C. Bellcrank system design guide</b>	<b>91</b>
C.1 Overview . . . . .	91
C.2 Step by Step guide . . . . .	92
<b>Appendix D. Bellcranks manufacturing</b>	<b>97</b>
<b>Bibliography</b>	<b>101</b>
<b>Index</b>	<b>102</b>
<b>Vita</b>	<b>103</b>
<b>Appendix E. Drawings</b>	<b>104</b>

## List of Tables

4.1	Torsional stiffness values vs model used . . . . .	28
A.1	Test 1 results . . . . .	81
A.2	Test 2 results . . . . .	82
A.3	Test 3 results . . . . .	84
A.4	Test 4 results . . . . .	85

## List of Figures

2.1	Garage layout . . . . .	9
3.1	Digital torsional stiffness analysis . . . . .	10
3.2	Physical torsional stiffness analysis . . . . .	11
3.3	Double A arm . . . . .	12
3.4	Pushrod suspension . . . . .	12
3.5	Pullrod suspension . . . . .	13
4.1	2017 chassis. . . . .	15
4.2	Original 2018 frame prototype . . . . .	16
4.3	Uncombined beams due to curvature . . . . .	19
4.4	Cover supports . . . . .	20
4.5	Free beam . . . . .	21
4.6	Suspension mounts . . . . .	21
4.7	FOS plot for 2017 frame . . . . .	22
4.8	Mesh, joints, forces and fixtures for Static test 1 . . . . .	23
4.9	Displacement plot of the first frame reconstruction simulation . . . . .	24
4.10	Front and rear roll hoops (light blue) . . . . .	25
4.11	Original front roll hoop vs modified front roll hoop . . . . .	25
4.12	Definitive Torsional stiffness model . . . . .	29
4.13	Torsional stiffness vs force . . . . .	30
4.14	Lateral view of the original 2018 frame . . . . .	31
4.15	Configuration 1 and configuration 2 of 2018 frame . . . . .	31
4.16	Original, configuration 3 and configuration 4 of 2018 frame . . . . .	32
4.17	Final design of 2018 frame . . . . .	33
4.18	2018 frame manufactured . . . . .	33
5.1	Bellcrank system . . . . .	34
5.2	2017 Bellcranks . . . . .	35

5.3	Suspension system of a vehicle . . . . .	35
5.4	Different ride frequencies plot . . . . .	36
5.5	Dynamic Reference Sketch and Equations . . . . .	38
5.6	ARB of a Formula 3 . . . . .	39
5.7	2017 Nosecone . . . . .	39
5.8	Traditional Design Methodology . . . . .	40
5.9	Topological optimisation design methodology . . . . .	41
5.10	Complete rear suspension dynamic sketch (left) and Bellcrank dynamic sketch (right) . . . . .	42
5.11	Coplanarity in bellcrank design . . . . .	43
5.12	Rear design space assembly . . . . .	44
5.13	Rear design space clearance assembly . . . . .	44
5.14	Rear design space and rear suspension assembly . . . . .	45
5.15	Solid Thinking Inspire refined design space . . . . .	46
5.16	Original orientation of Solidthinking plains . . . . .	48
5.17	Solid Thinking planes after applying Euler's rotation. . . . .	49
5.18	Topological optimized bellcrank . . . . .	50
5.19	RBC design configuration . . . . .	51
5.20	definitive RBC desing . . . . .	51
5.21	RBC position in the complete assembly . . . . .	52
5.22	Front Bellcrank System location . . . . .	53
5.23	Rear Bellcrank system model . . . . .	54
5.24	Sensor location in RBC motion study . . . . .	57
5.25	Rear Installation Ratio variation with wheel travel . . . . .	58
5.26	2017 front bellcrank system . . . . .	58
5.27	Planar configuration . . . . .	59
5.28	Hybrid configuration . . . . .	60
5.29	Improved Bellcrank configuration . . . . .	60
5.30	Front bellcrank design space . . . . .	61
5.31	Front IR variation with wheel travel . . . . .	61
5.32	FOS plot for ARB . . . . .	63
5.33	Front bellcrank topological optimization . . . . .	63

5.34	Front bellcrank CNC model . . . . .	64
5.35	2018 Front Bellcrank . . . . .	64
5.36	Front bellcrank system . . . . .	65
6.1	Budget . . . . .	67
7.1	Carbon fibre monocoque . . . . .	74
7.2	SLM process . . . . .	75
A.1	Modification 1.1 . . . . .	79
A.2	Front top section of the internal combustion team . . . . .	80
A.3	Alternative lateral configuration . . . . .	80
A.4	Modification 3.2 . . . . .	83
A.5	Modification 3.4 . . . . .	83
B.1	Original orientation of Solidthinking plains . . . . .	86
B.2	SolidWorks reference system and point parameters tools . . . . .	87
B.3	Nodal line, nutation angle, ground reference system and body's reference system . . . . .	88
B.4	Precession, nutation, and reference systems . . . . .	89
B.5	Spin, nutation, precession, and reference systems. . . . .	89
B.6	Euler's angle rotation to align reference systems . . . . .	90
B.7	Solid Thinking planes after applying Euler's rotation . . . . .	90
D.1	Original aluminum prism . . . . .	97
D.2	Saw . . . . .	98
D.3	Facing machine . . . . .	99
D.4	CNC boxes . . . . .	99
D.5	Final Front Bellcrank . . . . .	100
D.6	Final rear bellcrank . . . . .	100



# Chapter 1

## Introduction

This research is aimed to improve two subsystems of Formula SAE Electric single-seater. The Formula SAE Electric is a North American competition in which teams formed by students from prestigious universities build an electric racing car from scratch. The teams have to build a new car each year and then ship the car to where the competition takes place. Each car will be tested by a jury composed of experts from different automotive companies in different fields, such as design innovation, cost efficiency, endurance, and acceleration. This paper is focused on improving the mechanical systems of the racing car known as the chassis and the suspension.

### 1.1 Chassis

The first part of this research is focused on improving the 2018 prototype of the chassis. The 2017 chassis was a copy of the Internal Combustion (IC) FSAE team, which is the other FSAE competition where UT Austin participates. This team was created in 1981 and is one of the founders of the FSAE competition [6]. The IC team helped to adapt their chassis to the electric needs of last years car, creating a resistant but overweight design. The first step in this research was to make last years CAD model of the frame suitable for Finite Element Analysis

(FEA). Once the model was ready for FEA, its torsional stiffness will be calculated and used as an upper boundary for the 2018 chassis. The torsional stiffness is a measure of how many torque is needed to twist the frame one degree and is used as a rigidity measure for chassis in the automotive industry. The same process will be followed for the 2018 chassis prototype, and once the torsional rigidity is calculated, several design modifications will be tested in order to achieve the desired value of torsional stiffness while minimizing the weight.

## 1.2 Suspension

The final part of the research consists in improving both front and rear suspension systems. The geometry of the A-arms has been already determined by the team, so the challenge was to include the bellcrank system to each existent suspension in order to achieve the desired Installation Ratio (IR) and maintain clearance. The IR is a measure of how much does the shock compress by unitary wheel travel and is critical for how the car interacts with bumps and for maneuverability.

First, the bellcrank system is going to be created using 3D sketches in order to calculate the IR and to simplify the design iterations. Once an acceptable value is obtained, an assembly with the actual suspension parts and the frame will be created and used to check for clearance during the whole wheel travel. This will determine the relative position of each component of the bellcrank system and the maximum volume that the bellcrank can have without intersecting with other parts. This maximum volume is called design space, and it is going to be used for applying topological optimization for the bellcranks. Topological optimization is a design

technique that optimizes the geometry of a part with a known set of forces and constraints to minimize its mass while keeping a minimum specified factor of safety. The part generated by the topological optimization will be refined and adapted for manufacturing with a 3-axis CNC machine.

As most of the team is formed by undergraduate students, a step by step guide is going to be developed in order to help the next year students to design the bellcrank system quicker. This will allow the team to focus on other problems and to improve existing designs.

## Chapter 2

### Customer information

#### 2.1 Background of need

The SAE International Formula SAE program is an engineering design competition for undergraduate and graduate students. The competition provides participants with the opportunity to enhance their engineering design and project management skills by applying learned classroom theories in a challenging competition. The engineering design goal for teams is to develop and construct a single-seat race car for the non-professional weekend autocross racer with the best overall package of design, construction, performance, and cost [4].

The concept behind Formula SAE is that a fictional manufacturing company has contracted a design team to develop a small Formula-style race car. The prototype race car is to be evaluated for its potential as a production item. The target marketing group for the race car is the non-professional weekend autocross racer. Each student team designs builds and tests a prototype based on a series of rules whose purpose is both to ensure onsite event operations and promote clever problem-solving [4]. The vehicle will be inspected in a series of tests to ensure it complies with the competition rules; in addition, the vehicle with driver will be judged in a number of performance tests on track. The rest of the judging is completed by experts from motor-sports, automotive, aerospace and supplier industries

on student design, cost and sales presentations. LongHorn Racing Electric represent the University of Texas at Austin in this competition. The team was created in 2014 but two years ago all senior members quit, leaving the team with just freshman and sophomore students.

As the team was not able to perform Finite Element Analysis in the chassis last year, their frame was almost equal to the internal combustion Long Horn Racing Team. The electric formula SAE does not have an engine but a battery and a motor, so the chassis was heavier than required and not optimized for these systems. With proper analysis and FEA application, the new frame could be as resistant as last years model, but lighter. The team also want to improve its actual front bellcrank system to improve packaging and include an Anti Rollbar. The components of the rear suspension have not been optimized in weight, creating an unsprung mass that was excessively high. The team is also interested in researching new design techniques for sensitive parts, such as the bellcranks.

## **2.2 Customer Needs Statement**

Longhorn Racing Electric need to keep improving their current race car. In order to achieve this goal, several subsystems of the car need substantial modifications. The team needs to be able to use Finite Element Analysis in their both 2017 and 2018 chassis in order to make logical design modifications. The front suspension is going to be redesigned and the rear suspension needs to be optimized. All the unsprung mass needs to be analyzed and reduced to improve maneuverability.

## 2.3 Vehicle requirements

The global vehicle requirements for the 2018 vehicle were jointly set by the sub-system leads. In order to achieve the median performance values desired, the required longitudinal and lateral acceleration capabilities of the vehicle were set to 0.86 Gs and 1.5 Gs respectively. These values were derived from the scores and times seen in the acceleration and skidpad events. The desired weight distribution was set to 50-50 front-rear and 50-50 left-right. This was to balance oversteer and understeer effects, as well as to evenly spread the wear on the tires.

Due to time and space constraints at the competition, it was deemed necessary to quickly and easily maneuver and transport the accumulator. Overall packaging goals were centered around the accumulator and human interface. This drove the geometry of the frame behind and in front of the main roll hoop respectively. In addition, the differing environment at the airpark and differing preferences of the drivers necessitated the adjustability of several suspension parameters.

## 2.4 Functional Requirements

The primary goal of this design project will be to improve the general performance of the vehicle by improving the different subsystems that create the car. Each subsystem has different customer requirement:

- Acceleration 4.2 sec to 60 mph
- Skid pad 5.5 sec
- Autocross 58.9 sec

- Endurance 1520.6 sec
- Fuel Efficiency 0.612 gallons/sec
- Weight 500 lbf

## **2.5 Long Horn Racing Electric working methodology**

The team has a very structured and organized way of working. The team is structured as follow:

- The president of the team is Patrick McCabe, who supervise and coordinate design, manufacturing, and business.
- The design lead is Alex Choi, who is in charge of overseeing all the design sub-teams and make sure that all parts are well designed and fit accordingly with each other.
- Sam Snell is the Body lead and he is in charge of the frame and the body.
- Benji Eaton is the Dynamic lead, and he oversees suspension, steering, braking and tire assembly.
- James Yoder is in charge of all the electronics.
- John Cong is in charge of the powertrain.
- Nikunj Majmudar is in charge of the batteries.
- Amir Downing is responsible for manufacturing.

- Gijs Landwehr is the business lead.

Each one of the sub-teams is formed by 10 to 15 students, which they work designing different parts. Coordination between students is crucial, so the team mainly uses two coordinating programs:

- Slack: This is a professional program used to communicate within a company. It is a chat, divided into several channels. The most important is the general one, where announcements are posted. Each student has access to all chats but can only post in the one related to its sub-team.
- GrabCad: This program is a cloud storage for CAD files. Similar to CREO Windshield, it allows students to download CAD files from the cloud, work on them and then push the new version back up. It saves all the version in case there is a problem. The team uses a special code for the parts name: YY-SUB-ABCD RevN (Part Description), where
  - YY is the year of competition (18, 19, etc)
  - SUB is the sub-team for which the part belongs (DYN for dynamics)
  - A is the subsystem (1 is suspension, 2 steering, 3 wheel assembly)
  - B is the subassembly (A-arms, wheels, etc)
  - CD is the individual part number, in order of their creation (01, 02, 03)
  - 00 is reserved for the assembly itself
  - RevN is the revision number (Rev1, Rev2)



- Part Description, or common part name (Bellcrank)

The whole team meets every Sunday from 9 am to 7 pm, where all members work together in the same building. Each sub-team has a daily meeting, where students present their improvements or ask questions. Whenever there is a major concern about any part, Dr. Ronald Matthew can be consulted. After finalizing any major design, a design review need to be passed. This is done by the designer, the design lead, and the sub-team lead. If the design is validated the designer needs to meet with the manufacturing lead to see how to implement the design into a manufacturable part. The working space is depicted in figure 2.1:

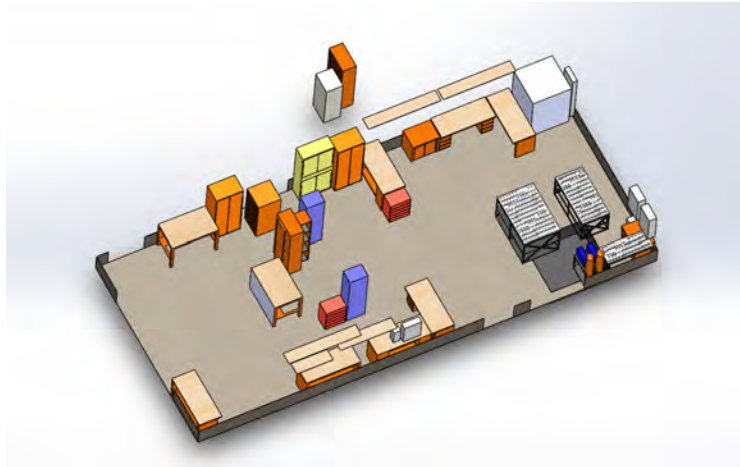


Figure 2.1: Garage layout

## Chapter 3

### State of the art

#### 3.1 Frame

The process of measuring the torsional stiffness of a racing car frame is very standardized. There are 2 main procedures that can be followed:

- Digital measurement: If the team has a CAD frame model, it is possible to use Finite Element Analysis to simulate a torsional stiffness test as shown in figure 3.1. It is required that the CAD model of the frame can mesh. This method is cheaper, less time consuming and can be done before manufacturing, which allows to improve the design of the frame by repeating the test several times after each modification.

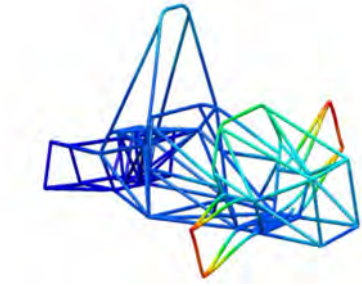


Figure 3.1: Digital torsional stiffness analysis

- Physical measurement: Once the frame is built, the torsional stiffness can be measured by fixing the rear of the frame and applying a torque to the

front. This can be done in several ways depending on the resources of each team. Figure 3.2 shows how the FSAE team of the Cooper Union University determined the torsional stiffness of its frame [1].

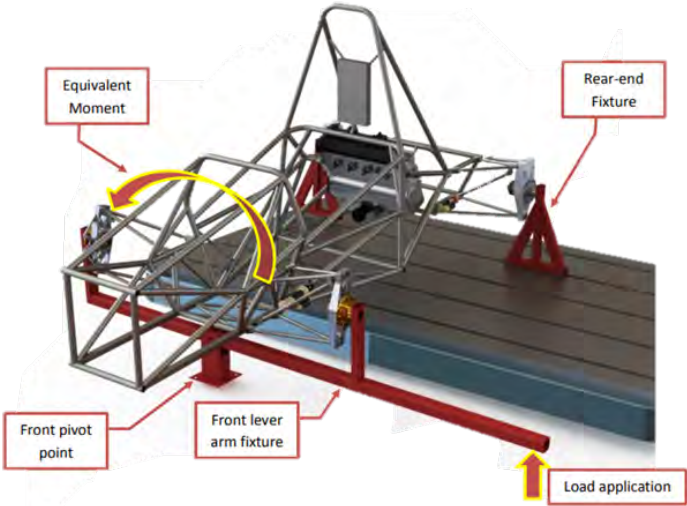


Figure 3.2: Physical torsional stiffness analysis

Ideally, a Formula SAE has to do both methods. The digital method has to be used in the design phase in order to allow for design modifications while monitoring the torsional stiffness value. The physical measurement is used to check that the frame manufactured behaves like in the simulations.

### 3.2 Suspension

There are several types of suspension geometries, however, the double A-arm suspension has become a standard for racing cars. It is used because of the broad variety of configurations that it offers, like adjustable camber and caster, and because of its reduced weight. It is also optimal for packaging and mounting. A

typical Double A-arm configuration can be seen in figure 3.3.



Figure 3.3: Double A arm

Regarding the bellcrank/shock system, there are two main configurations that works well with the Double A-arm configuration:

- Pushrod suspension: In this configuration, there is a rod called "pushrod" that connect the lower A-arm with the bellcrank. In this case, when the suspension goes up or has positive travel the shock experience compression. Figure 3.4 depicts this type of system.

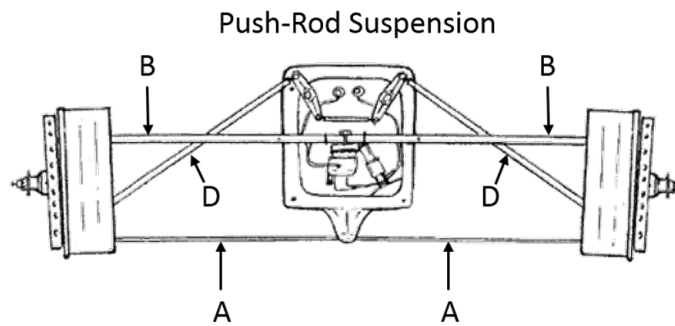


Figure 3.4: Pushrod suspension

- Pullrod suspension: In this case, the rod connects the upper A-arm with the bellcrank, which causes that the shock compress when the suspension goes down or has negative travel, as shown in figure3.5

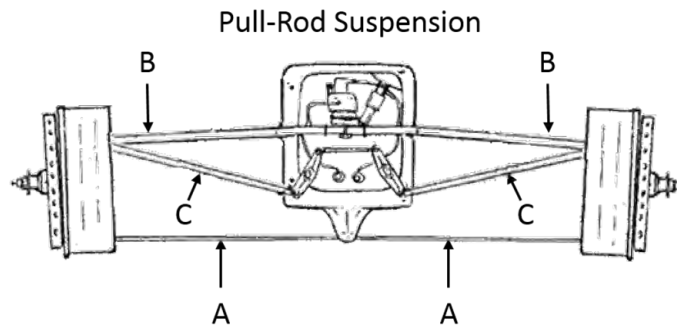


Figure 3.5: Pullrod suspension

Both bellcrank systems are equivalent, and the use of one or another is determined by packaging. The configuration that allows the desired installation ratio to be achieved while maintaining clearance with other parts is going to be chosen. However, the pushrod is the predominant type of suspension in most racing cars.

## Chapter 4

### Frame Design

#### 4.1 Chassis

A chassis, or a frame, is a structure made up of beams. It is one of the most important sub-systems of an FSAE car because it is accountable for the majority the weight of the single seater. Improving its design and efficiency have direct effects in handling, acceleration and fuel efficiency. Its main functions are:

- Protecting the driver in the case of an accident.
- Holding all subsystem together.

#### 4.2 Previous work

The 2017 chassis was designed for simplicity, robustness and manufacturing. Drawing heavily from advice from Longhorn Racing IC, the chassis is very similar to an existing internal combustion chassis, with modifications to allow for an electric drive system, accumulator, and the extra weight. The chassis is comprised of mostly 1-inch diameter tubing and deviates very little from the given tube sizes. The accumulator bay, previously engine bay, was enlarged and reinforced. The rear box was also triangulated and, in some parts, thickened to contain the motor and spool. Some of the front tubes supporting the suspension points were also thickened or

reinforced.

As the team has never realized any analysis in the 2017 frame (Figure 4.1), the first step in the design process was to make the last year CAD chassis model suitable for Finite Element Analysis (FEA). The team stated that they tried to run a static analysis without success due to mesh problems.

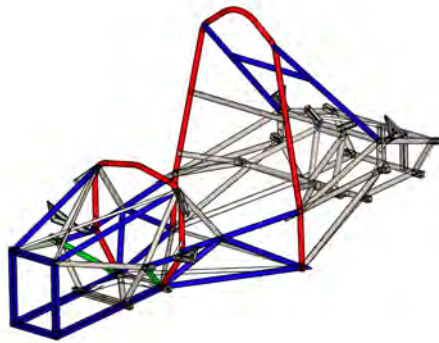


Figure 4.1: 2017 chassis.

### 4.3 Design objectives

The 2018 frame design started in June 2017. This research started in September when the frame was almost finished as depicted in figure 4.2. The frame was designed just to accomplish the Rulebook and to hold all the components in their place.

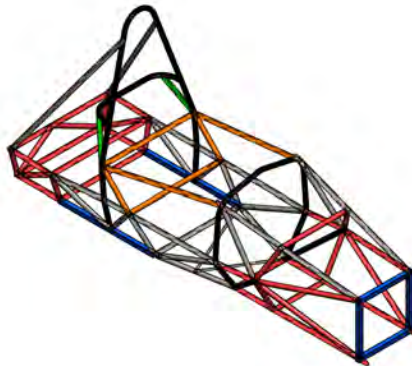


Figure 4.2: Original 2018 frame prototype

The Body Lead, Sam Snell, specified a set of design objectives that the design modifications should accomplish:

- Make the model FEA suitable
- Minimize weight
- Torsional stiffness value as close as possible to 1500 lbf-ft/deg.

Torsional stiffness is a measurement of how much torque is needed to twist the frame one degree. This torsional stiffness value is approximately 10 times stiffer than the torsional stiffness of the suspension [7]. The exact number for the torsional stiffness was given by Carrol Smith to the UT FSAE president. Carroll Smith (1932-2003) was a successful professional race car driver, engineer, and author. He wrote several race car engineering books as Tune to Win.

Another important design objective is to meet the requirements of the FSAE



competition regarding safety. The geometry and location of some beams are specified by the organization and are shown next [3]:

- Front Bulkhead A planar structure that defines the forward plane of the Major Structure of the Frame and functions to provide protection for the drivers feet. Tubes need to be square and 1 inch x 1 inch x 0.047 inches (dimensions of the square exterior wall and thickness).
- Front Bulkhead Support. Tubes need to be round and 1 inch x 0.047 inches (diameter and thickness).
- Roll Hoops Both the Front Hoop and the Main Hoop are classified as Roll Hoops. The need to be round and 1 inch x 0.095 inch
- Side Impact Structure The area of the side of the car extending from the top of the floor to 13.8 inches above the ground and from the Front Hoop back to the Main Hoop. The tubes need to be Round 1.0 inch (25.4 mm) x 0.065 inches (1.65 mm)
- Drivers Restraint Harness Attachment needs to be Round 1 inch (25.4 mm) x 0.065 inches (1.65 mm).
- Front Roll Hoop Bracing needs to be Round 1 inch (25.4 mm) x 0.065 inches (1.65 mm).
- Main Roll Hoop Bracing needs to be Round 1 inch (25.4 mm) x 0.065 inches (1.65 mm).

- Main Roll Hoop Bracing Supports The structure from the lower end of the Roll Hoop Bracing back to the Roll Hoop(s) needs to be Round 1.0 inch (25.4 mm) x 0.047 inches (1.20 mm).
- Shoulder Harness Mounting Bar is going to be Round 1.0 inch (25.4 mm) x 0.095 inches (2.4 mm).
- Shoulder Harness Mounting Bar Bracing Round 1.0 inch (25.4 mm) x 0.047 inches (1.20 mm)
- EV: Accumulator Protection Structure Round 1.0 inch (25.4 mm) x 0.065 inch (1.65 mm)
- EV: Tractive System Components Protection Round 1.0 inch (25.4 mm) x 0.047 inch (1.20 mm)
- Impact Attenuator A deformable, energy absorbing device located forward of the Front Bulkhead.

#### 4.4 Design methodology

The next steps summarize the design process of the modifications for the 2018 frame. This approach was used in order to maximize the robustness of the design:

- Make 2017 frame FEA suitable and measure its torsional stiffness. This value of torsional stiffness is going to be used as an upper limit, as the last years' frame did not break.

- Make 2018 frame prototype FEA suitable and measure its torsional stiffness. Test the consistency of the model and the robustness of the value obtained.
- Design modifications of 2018 frame in order to acquire the desired torsional stiffness value while minimizing weight increase.

#### 4.5 Torsional stiffness calculation for 2017 frame

The CAD model of 2017 chassis was not suitable for FEA. The main problem was that SolidWorks was not able to render the beam elements of the mesh for an unknown reason. The process followed to debug the frame model is shown next:

1. For an element to be treated as a beam element, it needs to be at least 10 times longer as it is thicker. There were several beams that were not combined due to their curvature, being three different members as shown in figure 4.3. There were 8 beams that presented the same problem. This was solved using the combine feature in SolidWorks as they should be part of only one beam originally.

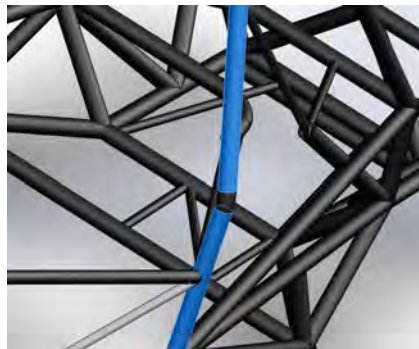


Figure 4.3: Uncombined beams due to curvature

2. All the beams that will not suffer any stress were removed in order to simplify the model. Figure 4.4 shows an example of this types of beams. In this case, there were meant to hold the cover of the car, and therefore they will not have any load on them. This will help to reduce the computational power required for meshing as it will also reduce possible errors due to excessive displacements.



Figure 4.4: Cover supports

3. There was a beam (Figure 4.5) that was not attached to any part of the frame, so it was not included in the analysis. It was a bar situated below the rear end of the chassis. Its purpose was not clear for any team member, so it was just excluded from the analysis, as it will not let the analysis work due to the lack of constraints.

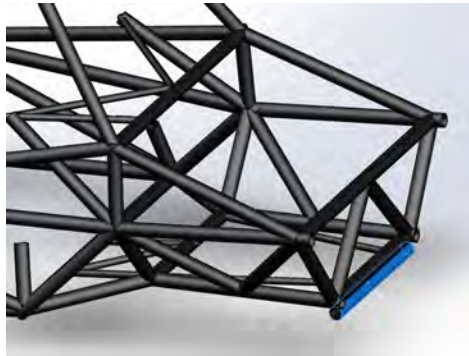


Figure 4.5: Free beam

4. Suspension mounts (Figure 4.6) were removed from the analysis, as they are solid bodies that will cause interference with the beams elements. SolidWorks tutorials for Formula SAE frame analysis states that fixing the nodes where the suspensions mounts meet the frame is an accurate approximation [9].

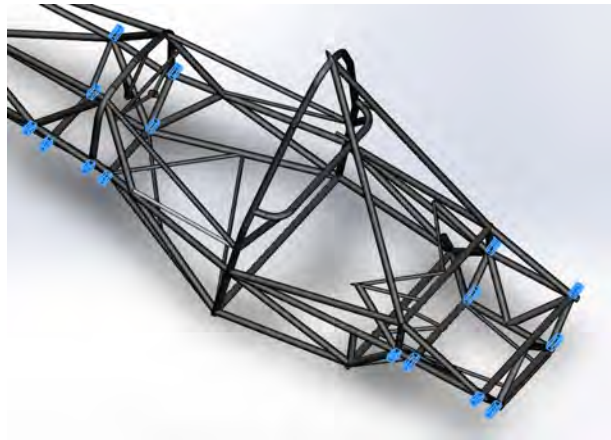


Figure 4.6: Suspension mounts

5. There were some hiding items that were causing the problem due to excessive displacements. The steering rack and the steering rod should be suppressed

for this model, but they were only hidden. Suppressing them from the analysis finally let the model to properly mesh and avoid the model to be unconstrained.

The next step consisted in applying forces and constraints. The end of the frame was fixed using the fixed geometry feature, and two opposing forces were applied in the front suspension joints, where the suspension mounts are. In order to obtain the first analysis and to see that everything was working, a standard value of 2500 N was applied in each front suspension mount. As the value of the force is not important for the torsional stiffness, a reasonable force value was estimated. The factor of safety plot is shown in Figure 4.7. The minimum FOS was 1.76 and max displacement was 4 mm. Both numbers are within an acceptable and logical order of magnitude, proving that the model is reliable.

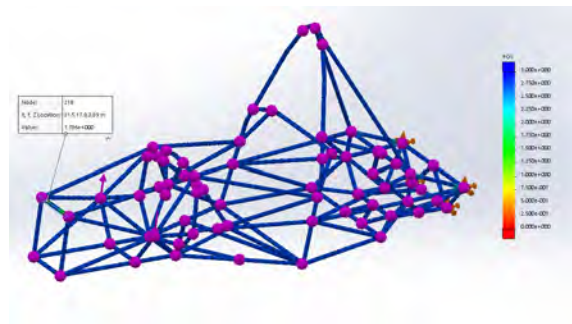


Figure 4.7: FOS plot for 2017 frame

A Torsional Stiffness analysis was developed using the combustion team excel tool. The tool required to input the vertical displacement of the points where the force was applied, distance of the force application point to the center-line of the car and the value of that force. The weight was obtained using the measure tool of

SolidWorks. These values were used as a reference for the future model:

- Weight: 88 pounds
- Torsional stiffness: 1900 lbf-ft/deg

## 4.6 Torsional stiffness calculation for 2018 frame

### 4.6.1 Preparation of 2018 model for FEA

In order to obtain a value for the torsional stiffness of the chassis, first, it is required to modify and improve the 2018 prototype model to be able to run Finite Element analysis. First, a simple static simulation was created. The model meshed without further problems. The rear end of the frame was fixed and opposing forces were applied to the front upper suspension mounts, creating a torque. This can be observed in Figure 4.8.

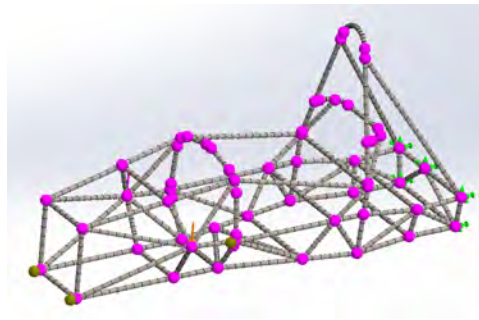


Figure 4.8: Mesh, joints, forces and fixtures for Static test 1

The model was not able to run the simulation due to the improper orientation of a beam element. All the beam elements were revised, suppressing or combining the elements that weren't long enough to be a beam element as did with the 2017 frame

model. The quality of the mesh was increased to the maximum and non-structural elements were removed, but the model still failed due to improper beams orientations. After several days of trials, it was obvious that the reason why the model was not FEA suitable was complex. In order to discover the misoriented beams or any other problem, the whole model was reconstructed. Small sections were redesigned, running test simulations each time to see at what point the simulation fails. Figure 4.9 depicts the simulation of the first part of the frame reconstruction process.

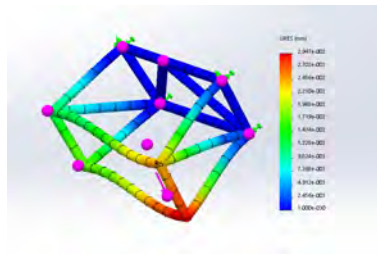


Figure 4.9: Displacement plot of the first frame reconstruction simulation

The whole frame was redesigned using that method. Thanks to this technique, the problem was finally detected. The front and rear roll hoops (light blue in Figure 4.10 ) were the ones producing the error.



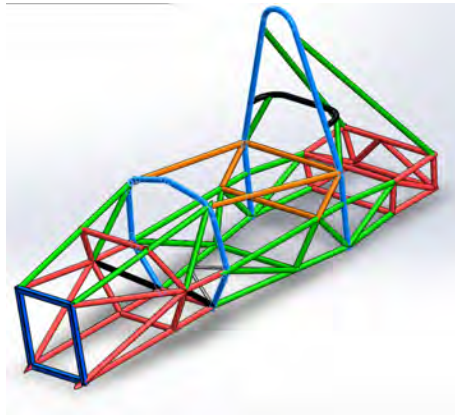


Figure 4.10: Front and rear roll hoops (light blue)

The actual problem was that these hoops were made of long beams that join small ones slightly curved for manufacturing purposes. Other problem detected was that beams should meet in the nodes in a logical way. Some nodes of the 2018 prototype what sharp edges that caused errors. For the Finite Element Analysis model, these small beam elements were removed as shown in Figure 4.11 and each problematic node was refined. The same process was applied to all the beams and nodes with the same characteristics, and the model finally was ready for simulations.

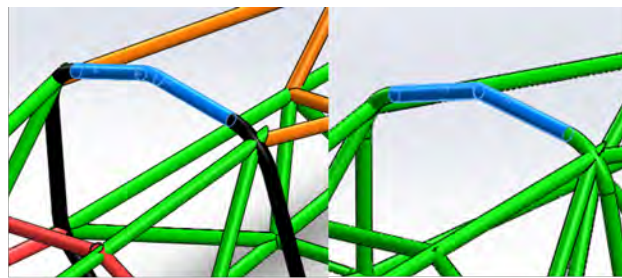


Figure 4.11: Original front roll hoop vs modified front roll hoop

#### 4.6.2 Torsional stiffness accuracy

In order to measure the torsional stiffness, front and rear suspension models were created, as these will apply forces and constraints in a more realistic way than the bare chassis itself. Both suspensions haven't been fully designed yet, so approximate models were used based on the dynamics sketches used for vehicle dynamics calculations. Several suspension models and fixture locations were tested, being the most important the one shown in the table 4.1. The models used can be divided into two different categories:

- Suspension model accuracy: Some of the model used tested the influence of having a suspension model as accurate as possible versus just using the suspension as a place to apply forces and fixtures. It was concluded that the complex suspension model created issues due to small beams that were not suitable for beam elements and that if the suspension model is made of beams, it will influence the value of the torsional stiffness of the frame due to the extra bending suffered by the suspension model. To avoid that, SolidWorks has truss elements, which are beams that cannot experience bending, just transmitting forces. Conclusion: Suspension model must be as simple as possible and made up of trusses.
- Position of the fixtures: Several locations for the fixtures were tried in order to see how they influenced the torsional stiffness. Initially, the model was fixed in the rear suspension, fixing the upper and lower parts of the upright model. Then, with the more simplified suspension model that only offered one

possible fixture location, the third fixture needed to make the model stable was placed in the middle part of one of the beams that was closer to the theoretical axis of rotation of the frame and the front suspension, like the IC team did. Finally, the rear box of the frame was fixed. Conclusion: Fixing only the rear suspension in the upright model produced values of torsional stiffness that were too low and fixing the beam close to the axis of rotation produced values that were too high. Fixing the rear box was chosen not only for consistency but also because it will allow recreating this experiment once the frame is built easier. This also proves that the IC tool for calculating the torsional stiffness is not very accurate.

The conclusion obtained from all these simulations is that in order to obtain the torsional stiffness value for just the frame, the suspension model needs to be as simple as possible and it needs to be made of trusses, to avoid errors in the torsional stiffness measure due to bending of the suspension components. The fixtures had to be applied in the rear box of the frame, making the rear suspension model redundant.

Table 4.1: Torsional stiffness values vs model used

	Torsional stiffness (Nm/deg)
Complete rear suspension and simple front suspension no truss. 4 fixtures rear A arms.	1340.0
Simplified front and rear suspension, no truss, 4 fixtures back of rear box.	1636.1
Simplified front suspension, no truss, excluded rear suspension. 4 fixtures back of rear box.	1599.0
Simplified front and rear suspension, all truss, 4 fixtures back of rear box.	1609.4
Simplified front suspension, all truss, excluded rear suspension, 4 fixtures back of rear box.	1587.3
Simplified front suspension, all truss, excluded rear suspension, 2 fixtures at top back of rear box, 1 fixture between front a-arms.	1847.8
Complete rear suspension and simple front suspension no truss. 4 fixtures rear A arms.	761.2
Complete rear suspension and simple front suspension all truss. 2 fixtures rear A arms one middle low bar.	1285.3
long rear suspension box chassis with rear box fixed and front suspension arms as truss.	962.0

The definitive model that is going to be used is shown in Figure 4.12. The

force is going to be applied at the end of the front suspension arms model (pink arrows) and the end of the rear box is going to be fixed (green arrows). It can be seen that there is no rear suspension model as it was proven to be unnecessary in the previous paragraphs.

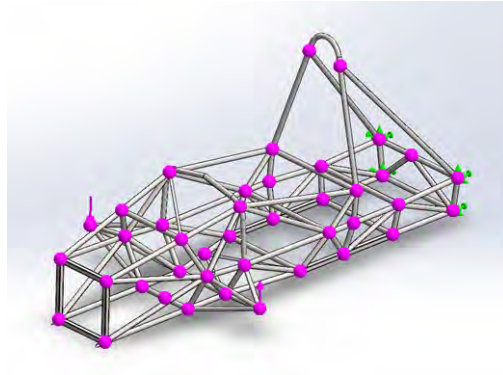


Figure 4.12: Definitive Torsional stiffness model

The next step for testing the reliability of the model is to test that the torsional stiffness value does not depend on the value of the forces/torque applied. One of the main problems faced during this phase of the research was that the team keeps doing modifications to the frame based on packaging and the rules of the competition. This forced to recreate the whole simulation model every week, as changes are impossible to predict because they depend on the other sub-teams. After the last modification, the model was rebuilt step by step as explained in section 4.6.1. Figure 4.13 shows the torsional stiffness values for different force values. It is concluded that the torsional stiffness value does not depend on the value of the force.

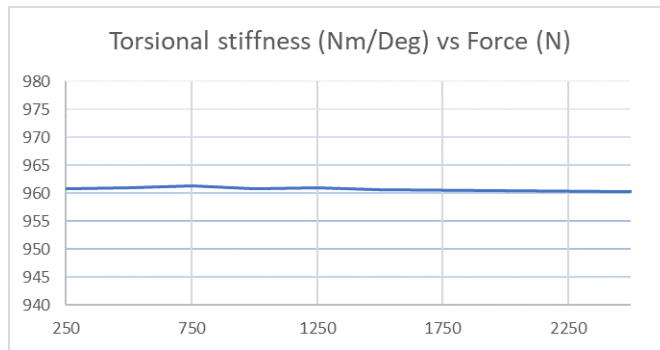


Figure 4.13: Torsional stiffness vs force

Then, some other modifications were made in the frame to support the firewall required by the rulebook, so the model needed to be rebuilt a third time. But this time it was the final modification confirmed by all sub-teams. Using the same suspension model and meshing techniques, a value of 1164 Lbf-ft/deg. was obtained for the final design of the frame. Its weight was 74.85 pounds, lighter than last year frame which weighed 87.4 pounds. The aim for the torsional stiffness is to be 10 times stiffer than the suspension stiffness, which is 149 Lbf-ft/deg. So, the objective torsional stiffness of the frame needs to be as close as possible to 1490 Lbf-ft/deg, as stated by Carrol Smith. As the initial value is lower, new tubes needed to be strategically added to the frame in order to increase stiffness while minimizing weight increase.

#### 4.7 Design modifications for 2018 frame

Different design approaches were tested in this section based on achieving full triangulation of the structure. The first design modification was focused on the

lateral side of the frame shown in figure 4.14.

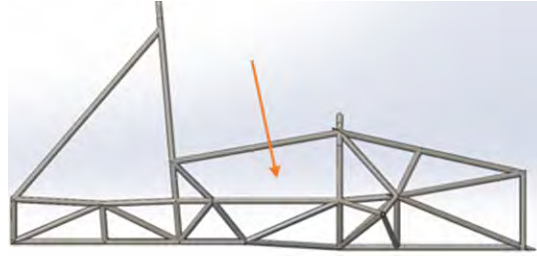


Figure 4.14: Lateral view of the original 2018 frame

Two different configurations were tested in order to achieve full triangulation, as shown in Figure 4.15. While the configuration on the right was lighter, the configuration on the left had an extra beam that made the installation of the protective fire panel easier.

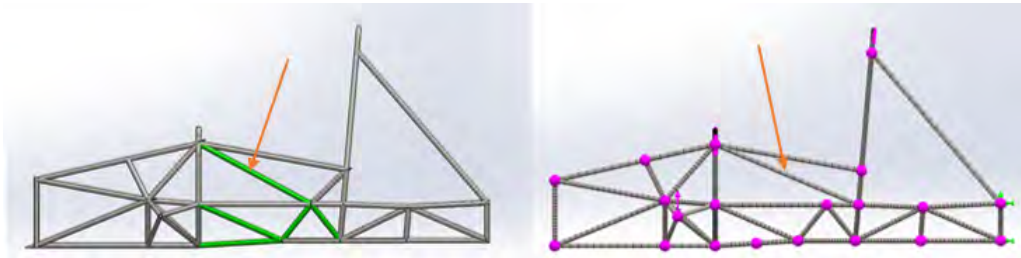


Figure 4.15: Configuration 1 and configuration 2 of 2018 frame

The other design modification was realized in the top part of the nose of the frame. As displayed in figure 4.16, the original configuration had two zones that were not triangulated. The two design modification are also shown below. Only one beam was added in the non-triangulated sections, as adding two beams forming a cross did not increase the torsional stiffness for the extra weight added.

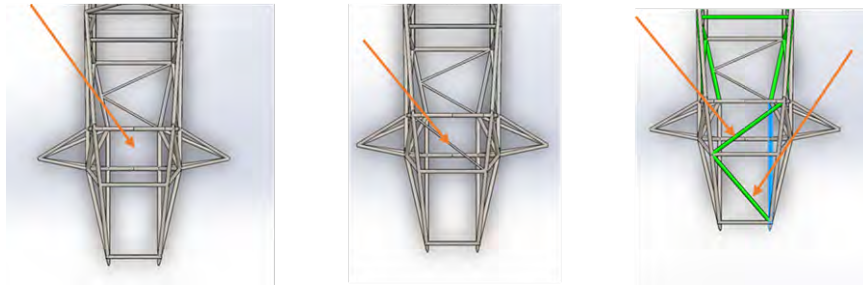


Figure 4.16: Original, configuration 3 and configuration 4 of 2018 frame

In order to obtain a value of torsional stiffness as close as possible to 1500 Lbf-ft/deg while minimizing the weight increase, all the configuration were tested individually and combined, while also testing different tube thickness. The tests were developed in 4 groups:

- Test 1: Lateral tube configurations
- Test 2: Lateral tube thickness
- Test 3: Front top configurations and thickness
- Test 4: Combination of both modifications

A comprehensive list of all configurations and tube thickness can be found in appendix A. The factor of safety was included in the test as a comparative measure. As the forces used were arbitrary, it makes no sense to use the FOS as a design indicator. However, it is useful to compare this value between configurations, to see if it increase in the same proportions as the torsional stiffness and the weight. After testing 17 different configurations, the final design is shown in figure 4.17. The



final torsional stiffness was increased a 33.87 % to 1557 lbf-ft/deg while the weight only increased a 2.42 % to 76.66 pounds. The final frame design of 2018 is 13 % lighter than last years.

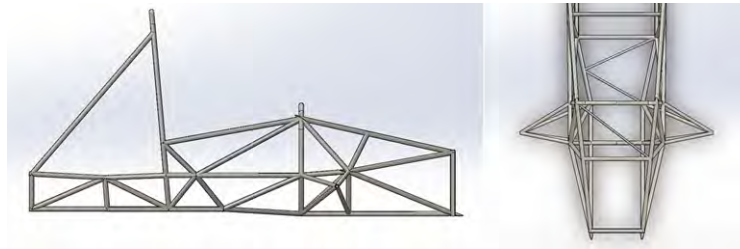


Figure 4.17: Final design of 2018 frame

Each beam was created as a separated SolidWorks part and trimmed in order to perfectly join in each node. The tubes were laser cut and welded in the shop by the team. The final manufactured chassis can be seen in figure 4.18.

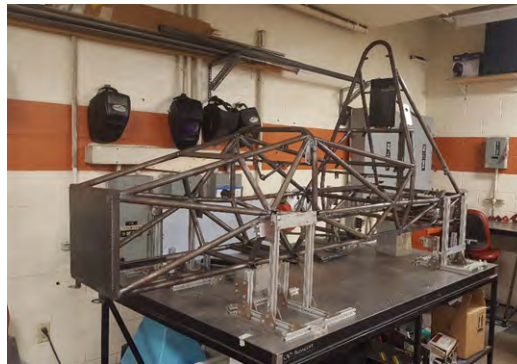


Figure 4.18: 2018 frame manufactured

## Chapter 5

### Bellcrank Design

#### 5.1 Bellcrank system

A bellcrank is a solid body which changes motion through an angle, by rotating about a point. The system is depicted in figure 5.1 and consists in the pushrod, the bellcrank itself, the shock and the antiroll bar (ARB). In a race car, bellcranks are in charge of:

- Transferring the forces generated by the pushrod and the ARB to the shock absorber.
- Defining the Installation Ratio, which is specified as unit shock compression per unit wheel travel. This ratio is very important for handling, as it is a measure of how the car rolls in corners.

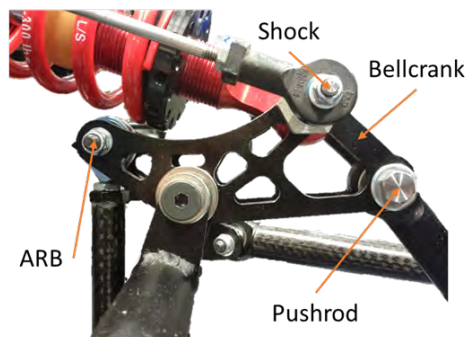


Figure 5.1: Bellcrank system

## 5.2 Previous work

2017 front and rear bellcranks are shown in figure 5.2. They were made of steel and the team has not performed any analysis on them. No Installation Ratio calculations were performed in these models, they were designed for clearance and durability.



Figure 5.2: 2017 Bellcranks

## 5.3 Installation ratio calculation for 2018 bellcranks

The installation ratio (IR) is defined as the shock compression per wheel travel and it is defined by suspension parameters. To calculate it, the first step is to select a shock and to be able to do that, a target ride frequency must be chosen. Ride frequency is the frequency at which a suspension system will resonate, as a suspension system is a series of two spring and mass system as shown in Figure 5.3.

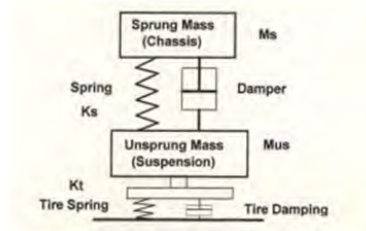


Figure 5.3: Suspension system of a vehicle

The formula SAE rulebook recommends a ride frequency at the front of 2.5Hz, and something between 5% and 15% higher ride frequency at the rear. Historically, all formula SAE had the same ride frequency both front and rear, but since the race track moved to Lincoln Airport, the bumpy nature of this track create the necessity of flat ride tuning (different ride frequencies). The different ride frequencies will let the rear catch up in amplitude with the front as a bump is hit, making the car move up and down the same amount in the front as in the rear. This is depicted in Figure 5.4.

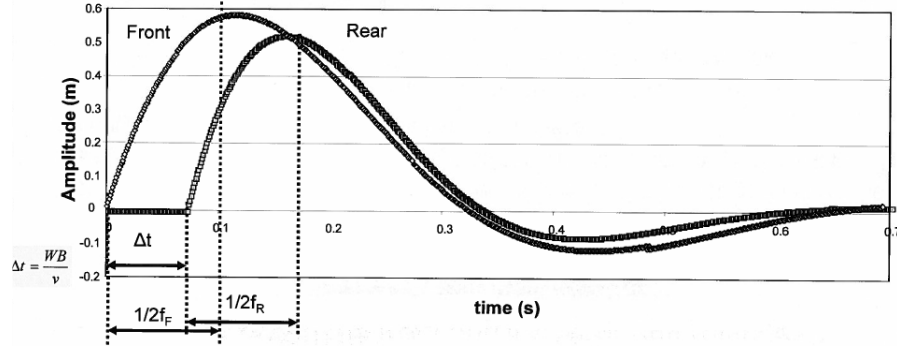


Figure 5.4: Different ride frequencies plot

Now it is crucial to obtain the best estimation as possible for the sprung and unsprung mass. The unsprung mass consists of all the car components that are under the shocks, such as the A-arms, the upright, the rim... With the unsprung mass and the ride frequency, we can obtain the ride rate, which is the vertical force per unit of vertical displacement of the tires ground contact patch with respect to the chassis, as shown in equation 5.1. The super index  $f$  refers to the front suspension and  $m$  to unsprung mass. This equation is analog for the rear suspension.

$$k_R^f = m_s^f(2\pi + m_{ride}^f)^2 \quad (5.1)$$

The next step consists in obtaining the wheel rate, which is the rate of the whole system including the tire. Tire rates are a known value (we are using the same tires as last year). Using equation 5.2 it is possible to obtain the wheel rates.

$$k_w^f = \frac{k_R^f k_t^f}{k_t^f - k_r^f} \quad (5.2)$$

The team dealt with the spring selection. According to equation 5.3, there are 2 degrees of freedom to obtain the desirable wheel rate for the chosen ride frequency. The installation ratio is the amount of compression in the shock by vertical movement of the wheel and the spring rate the amount of weight that is needed to compress the shock by one inch. As there are not infinite values of spring rates, engineers chose a value of the spring rates and then design the rocker plate or bellcrank to achieve the necessary installation ratio. The installation ratio was finally 0.67 for the Front Bellcrank and 0.8 for the Rear Bellcrank.

$$k_w = (IR)^2 k_{sp} \quad (5.3)$$

#### 5.4 Dynamic Reference Sketch

The team developed a tool called the Dynamic Reference Sketch (figure 5.5) in order to have all suspension parts referenced to the same origin. It is made of 3D sketches with geometrical relations and equations that allow to design and verify

different suspension parameters such as camber variations or anti squad. It is also useful to check for clearances if there is no powerful computer around, as assemblies require a lot of computational power. The design lead included an equation called Installation Ratio that was defined as the shock compression divided by the vertical displacement of the wheel. This equation gave back the value of the installation ratio for a specified wheel travel value.

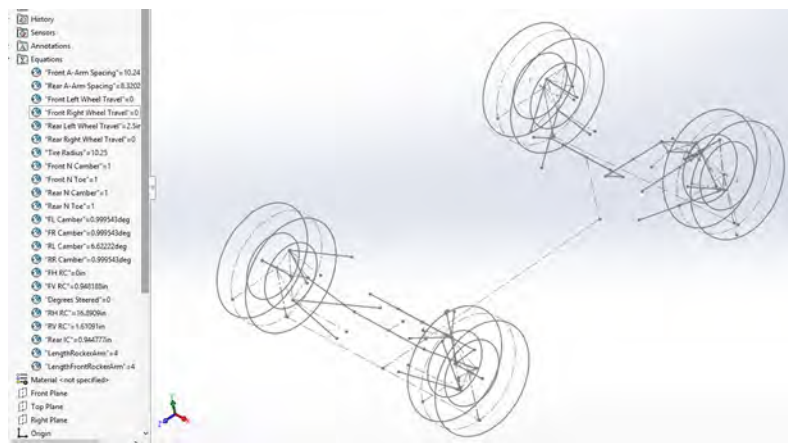


Figure 5.5: Dynamic Reference Sketch and Equations

## 5.5 Anti-roll bar (ARB)

The anti-roll bar is a torsion bar that connects the right and left bellcranks. By connecting both right and left suspension, it helps to reduce the amount of roll of the car. This is interesting because it allows having a softer suspension, which helps to absorb bumps better but avoids excessive roll in the corners that cause an uncomfortable handling feeling. Figure 5.6 depict the ARB of a Formula 3 single seater. The ARB here is not in torsion but in bending. The stress state of the ARB depends on the bellcrank configuration.



Figure 5.6: ARB of a Formula 3

## 5.6 Nosecone

The nosecone of a single seater is a body structure normally made of glass fiber or carbon fiber. Its main functions are: absorb energy in the case of a frontal collision and reduce the drag coefficient of the single seater. Its design is normally created using Computational Fluid Dynamics and it takes a lot of time to design. In figure 5.7 the nosecone can be seen.



Figure 5.7: 2017 Nosecone

## 5.7 Design objectives

The bellcrank needs to fulfill the following design specifications:  
High priority:

- Be able to support the forces applied without breaking.
- Minimize the weight.
- Avoid interference with existing parts.
- Be manufacturable with a 3 axis CNC machine.

Low priority:

- Maximize simplicity.
- Minimize price.

## 5.8 Design methodology

The traditional mechanical design approach consists in developing a concept design that satisfies your basic requirements, then detailed and develop simulations. According to the simulation outputs the design is modified until the desired simulation parameters, such as the factor of safety, are achieved. This lead to the optimal design as shown in figure 5.8.

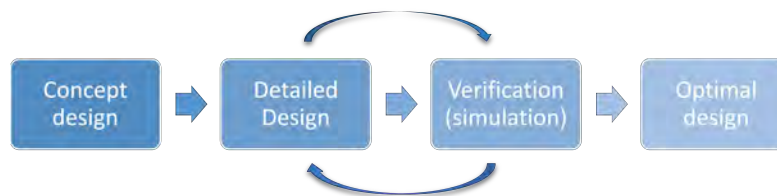


Figure 5.8: Traditional Design Methodology



However, for this design process, the topological optimization approach was used. This process starts with the creation of a design space, which is the maximum volume that a part can have without interfering with other parts and maintaining the design specifications. Then, this design space is introduced in a topological optimization software. SolidThinking Inspire was used as it is free for FSAE students. Then introducing the loads, fixtures and desired FOS the program generates the optimal geometry.



Figure 5.9: Topological optimisation design methodology

## 5.9 Rear Bellcrank Design Process

The first step was to create a bellcrank sketch in the DRS. As a design constraint was that all the forces needed to be as co-planar as possible, the bellcrank will be sketched in the plane created by the push rod mount in the Bellcrank, the chassis bellcrank mounting point (that will be in the top rear frame node for structural integrity) and the shock mount to the chassis, so all the center line of the shock will also be on the same plane as the other components. The Anti Roll Bar mounting was constrained by the clearance with the sock and minimum distance to the bellcrank frame mount. The lever arm of the ARB was designed to be in the bellcrank plane too. With all these constraints, a preliminary design of the bellcrank 3D sketch was created as shown in figure 5.10.

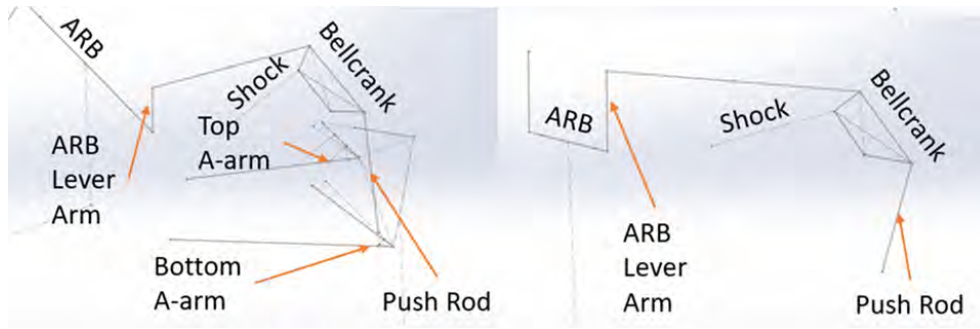


Figure 5.10: Complete rear suspension dynamic sketch (left) and Bellcrank dynamic sketch (right)

Then, the installation ratio equation was including in the global equations of the DYN REF sketch, as stated in equation 5.4. The next step was an iterative process where the Pushrod mounting point with the lower A-arm, the push rod bellcrank mounting point, the shock mounting point, and the shock mounting points were modified until the desired installation ratio was achieved. The iteration process was complex as each bellcrank geometry needed to be tested in maximum compression and extension in order to check that the installation ratio does not vary excessively with the wheel travel and that there was clearance enough between all the suspension members in each position. The final IR obtained was 0.8, due to clearance problems with the half shafts of the motor.

$$IR = \sqrt{\frac{k_w}{k_{sp}}} = \frac{\text{Shock compression}}{\text{Wheel travel}} \quad (5.4)$$

Once the shock mounting points and the push rod mounting points that best accomplish all the imposed restrictions were obtained, the ARB mounting point and ARB lever arms were determined, as the position of the ARB bar itself. Clearance

and co-planarity were the constraints imposed, with the minimum distance to the bellcrank frame mounting. To ensure co-planarity, the shocks were positioned in standard compression, supporting the cars own weight. A perpendicular line to the ground was drawn, cutting the beam center line where the ARB was going to be placed. This line will cut the bellcrank plane, determining the length of the lever arm for it to be co-planar in standard position. However, as the wheels move, the forces transmitted to the bellcrank by the ARB won't be co-planar, but the maximum angle measured was 3 degrees. The push rod has a maximum deviation angle of 6.2 degrees. Co-planarity is depicted in Figure 5.11.

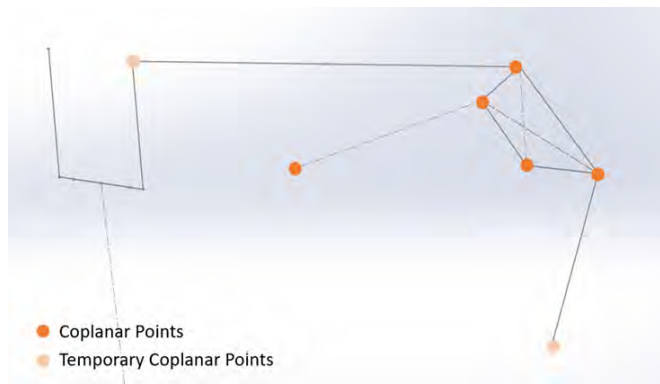


Figure 5.11: Coplanarity in bellcrank design

### 5.9.1 Design Space

The design space is defined as the maximum volume that a part can have without interfering with other elements. To obtain it, an assembly was created in SolidWorks, including a model of the two hinges of the ARB mounting and the push rod. For the shock mounting, a model was creating using Plane x and plane y that can be found in annex z. The assembly is depicted in figure 5.12, including the DRS.

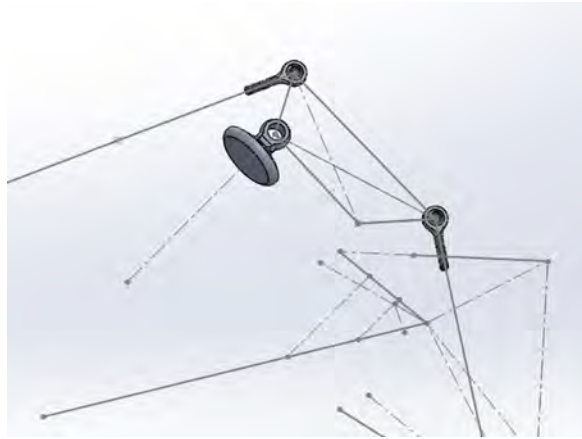


Figure 5.12: Rear design space assembly

The frame was also included in the assembly to check if the bellcrank interferes with any of the beams during its travel. The clearance assembly is shown in figure 5.13. Using the assembly as a reference, a new part was created to be the design space.

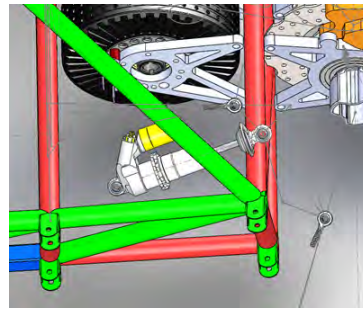


Figure 5.13: Rear design space clearance assembly

In order to achieve the desired installation ratio, the relative position of the shock mount, the push rod mound, and the frame mount were modified. As the wheel travel is not in the same plane as the shock, the influence of the relative

displacement of each mount in the IR was not trivial. Many iterations were needed in order to get as close as possible to the desired IR while maintaining clearance. The modification of the relative position of the amount required to first check the IR by averaging the IR value in maximum compression and maximum extension using the DRS and then check clearances in the assembly. After several iterations, a constant IR of 0.79 was achieved, very close to the desired 0.8. The final design space and the final rear suspension assembly with the design space are shown in figure 5.14.

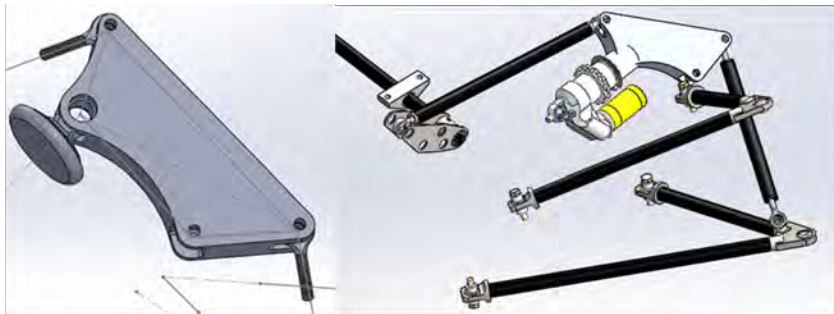


Figure 5.14: Rear design space and rear suspension assembly

### 5.9.2 Topological optimization

The design space needed to be exported as a Parasolid from SolidWorks, so no sketches can be used. The design space was refined by splitting the part into two solids, one solid being the 4 empty cylinders around the mountings where the optimization software will not optimize, and the rest of the design space that will be optimized. This is shown in figure 5.15. The topological optimization software requires forces and constraints as a regular Finite Element Analysis. As the ARB

forces and shock forces are easier to calculate, the push rod mount was fixed as a hinge, with the chassis mount (grey and red dots in figure 5.15).



Figure 5.15: Solid Thinking Inspire refined design space

Solid Thinking Inspire does not have the ability to import sketches, obtaining the orientation of the forces wasn't trivial. Inspire is not capable of creating planes or sketches outside of the part surface, it is mandatory to sketch in one of the parts faces and then rotating and moving the plane manually or imputing the exact amount that you want them to move. This constraint made working with the Inspire software very unpleasant. For the forces orientation, equation 5.5 was used in combination with the DRS to obtain the coordinates of the force vectors. The maximum forces will occur in maximum shock compression, which occurs when the wheel travel is at 2 inches. The DRS allows to set wheel travel to 2 inches and this will modify the position of all 3D sketches to simulate maximum compression. This allows pinpointing the end of each line representing each suspension components in order to obtain the coordinates of different points needed for the vector calculation.

$$\overline{AB} = \overline{OB} - \overline{OA} \quad (5.5)$$

The reference system of the design space created in SolidWorks matches the

car reference system so when it is exported as a Parasolid to Inspire, force vectors can be manually introduced in the software without any need of transformation. For the value of the maximum shock force, Equation 5.6 was used to obtain a value of 448.8 lbf.

$$k_{shock} = k_{sp} \quad x_{maxcomp} \quad (5.6)$$

For the maximum force applied by the ARB, the maximum torque that it can handle without breaking was obtained. The maximum torque of an Anti-Roll Bar is given by equation 5.7

$$T = \frac{J \quad \tau_{max}}{R_{max}} \quad (5.7)$$

Where T is Torque, J is the polar moment of inertia of area,  $\tau_{max}$  is the maximum shear stress that the material is capable to handle without breaking and R max is the distance from the center to the outer surface of the shaft. The bending produced by the force that will generate the torque is not accounted, as this will reduce the ARB max torque. We are calculating the torque in order to design the bell crank, so the objective is to find a worst-case scenario load with a safety factor. The Rear ARB is a hollow bar of 26 inches long, 0.63 inches of external diameter and 0.38 inch of internal diameter. The  $R_{ext} = 0.008$  meters,  $R_{int} = 0.00482$  meters and the polar moment of inertia of a hollow shaft is given by equation 5.8

$$J = \frac{\pi}{2}(r_{ext}^4 - r_{int}^4) \quad (5.8)$$

The material of the shaft is AISI 4130 steel, annealed at 865C, with a yield strength of  $3,6 * 10^8$  N/m. To obtain the maximum shear stress that the bar is capable to handle, the Von Misses stress criterion for pure shear will be applied. Equation 5.9 depict this criterion:

$$\sigma_v = \sqrt{3}\tau_{xy} \quad (5.9)$$

Combining all the equations, the maximum torque that the rear ARB is capable of handling 145 Nm or 1283 lbf-in. This torque divided by the lever arm creates a 428 lbf force in the bellcrank.

To make the bellcrank manufacturable in a 3-axis CNC machine it needed to be symmetric according to the themed plane. As the software does not has a feature to create symmetry planes automatically, by referring them to existing geometry, the original planes of the car reference systems needed to be rotated by hand to make the align with the part desired reference system. The problem now was to obtain the degrees that each reference plane needed to be rotated, and the order, for them to match the part reference system. Figure 5.16 depicts the initial orientation of the plains.

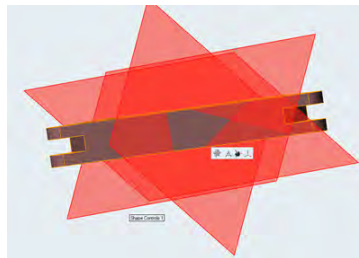


Figure 5.16: Original orientation of Solidthinking plains



In order to calculate the degrees needed, the inverse Euler's angle problem needed to be solved. A detail explanation of the process followed to calculate those angles is depicted in Annex B. After rotating each plane in order, the result is shown in figure 5.17

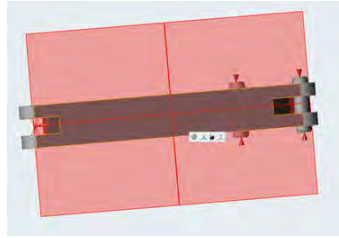


Figure 5.17: Solid Thinking planes after applying Euler's rotation.

Once the forces and the symmetry plains are introduced into the program, a safety factor needs to be specified. In racing cars, a usual factor of safety is 1.2 [7]. However, as the team does not have enough budget for prototyping and this is the first time using this design approach, a value of 2 was selected. It is also important to notice that the amount of weight saved from a FOS of 1.2 to a FOS of 2 is not comparable to the increase in resistance. The team is relatively new and the objective is to finish the race. The risk of using a FOS of 1.2 is not worth it. The results of the topological optimization are depicted in figure 5.18.



Figure 5.18: Topological optimized bellcrank

One important problem that this geometry presented was the absence of material between the two fixtures. As the program isn't very advanced, the only option available for cylindrical fixtures are fixed geometry and hinges. For the model to be static, two hinge fixtures were applied in the BC frame mount and in the push rod mount. This caused an absence of relative movement between hinges, which makes the program think that there is no material needed between those parts. The optimal geometry was also modified for manufacturing purposes. The part was divided into two halves to minimize its time in the CNC machine. Different geometries were tested to check the reliability of the topological optimization process, and the parts were both over a FOS of 2. Design configurations are shown in figure 5.19. The first one was finally used as the amount in weight saving was small in comparison with all the resistance gained.



Figure 5.19: RBC design configuration

### 5.9.3 Final rear bellcrank design

The final rear bellcrank design can be seen in figure 5.20:



Figure 5.20: definitive RBC desing

Figure 5.21 shown the complete rear bellcrank system located in the car assembly. The 2018 design has accomplished the following specifications:

- The Rear Bellcrank is 61% lighter.

- Has a constant Installation ratio of 0.79 through all wheel travel.
- During max compression and extension, the maximum angle that forces make with the bellcrank plane is 6.2 degrees.
- It has built in spacers that make mounting and dismounting easier.

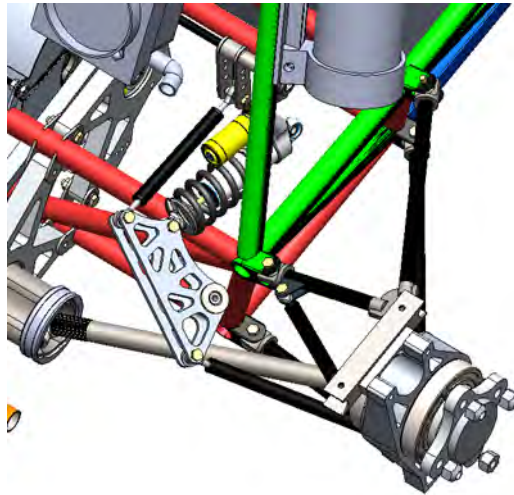


Figure 5.21: RBC position in the complete assembly

## 5.10 Front Bellcrank Design

The front bellcrank design process was more complex than the rear one due to the following factors:

- The Dynamic Reference Sketch was not working for the front bellcrank.
- The steering system and the nose cone were already designed and made packaging harder.

- There was no space for the anti-roll bar. Two students had been working on the design of the ARB and they were positive about the impossibility of fitting and ARB in the front suspension.

Figure 5.22 depicts the space in which the front bellcrank system needed to be placed, including the shock, the bellcrank, the pushrod and the anti-roll bar.

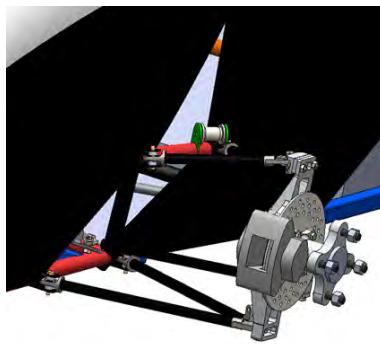


Figure 5.22: Front Bellcrank System location

### 5.10.1 Motion study

After spending weeks trying to fix the relationship problem between the 3D sketches of the Dynamic Reference Sketch that either over restrain the model or gave too many degrees of freedom, an alternative approach was taken.

The SolidWorks tool called Motion Study was used to substitute the Dynamic Reference Sketch. This tool allows parts in an assembly to move using virtual actuators according to the mates that each part has in the assembly. The first step for the motion study was to create models of each component of the front suspension in order to reduce the computational load required to operate the assembly.

Models of the lower A-arms and pushrod were created. A simplified model of the front bellcrank was also created. Models were created with a 3D sketch with limited relation or dimensions, which allows modifying the dimension of each component in order to adapt the design to the constraints, such as the installation ratio.

### 5.10.2 Motion study refinements

In order to validate this new methodology, a model of the rear suspension was created in order to see if it was possible to obtain the same measurement of the installation ratio. Figure 5.23 shows the simplified rear suspension model, in combination with the dynamic reference sketch that remained static.



Figure 5.23: Rear Bellcrank system model

Once the model assembly was created, it was introduced in the motion study. Then, an oscillating motor was placed in the lower A-arm and designed to create a wheel travel of 1 inch. The idea was to stop the model in the maximum compression of 1 inch and maximum extension of -1 inch and then measure the compression of the shock using the SolidWorks tool measure. However, whenever the motion study

was run, it does not recreate the desired movement. So, the first approach was to fix all the dimensions and relations of each model, which will make it more difficult to adjust when looking for a specific installation ratio. This improved the magnitude of the mistake but keep creating problems. After doing some research it was discovered that all sketches needed to be defined and that the problem was related to the integration method used by SolidWorks. The SolidWorks Motion solver offers three integration methods for computing motion [8]:

- The GSTIFF integration method developed by C. W. Gear is a variable order, variable step size integration method. It is the default method used by the SolidWorks Motion solver. The GSTIFF method is a fast and accurate method for computing displacements for a wide range of motion analysis problems.
- WSTIFF is another variable order, variable step size stiff integrator. GSTIFF and WSTIFF are similar in formulation and behavior. Both use a backward difference formulation. They differ in that the GSTIFF coefficients are calculated assuming a constant step size, whereas WSTIFF coefficients are a function of the step size. If the step size changes suddenly during integration, GSTIFF introduces a small error, while WSTIFF can handle step size changes without loss of accuracy. Sudden step size changes occur whenever there are discontinuous forces, discontinuous motions or abrupt events such as contact in the model.
- SI2\_GSTIFF, a Stabilized Index-2 method, is a modification of the GSTIFF method. This integration method provides better error control over the veloc-

ity and acceleration terms in the equations of motion. Provided the motion is sufficiently smooth, SI2\_GSTIFF velocity and acceleration results are more accurate than those computed with GSTIFF or WSTIFF, even for motions with high-frequency oscillations. SI2\_GSTIFF is also more accurate with smaller step sizes but is significantly slower.

The SI2\_GSTIFF integrator seems to improve error control over velocity and acceleration, so this was the one selected. After that, the simulations worked every time which allowed to measure the installation ratio, being this one the same as the one measured using the Dynamic Reference Sketch. While researching for the integrators another interesting feature was discovered. There is a tool called sensor, which allows obtaining the position of an element during the motion of the study. These sensors were placed on the wheel mount, which will measure the wheel travel, and two in the shock mount in the frame and in the bellcrank mount on the bellcrank. Sensor tool allowed to export the coordinates of each sensor through the motion to Excel. Figure 5.24 depicts the location of each sensor.



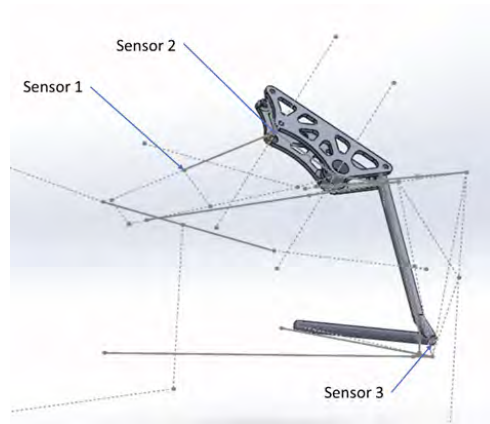


Figure 5.24: Sensor location in RBC motion study

The transformation realized in Excel were:

- Sensor 1 and Sensor 2 represented the two points of the shock. In order to obtain the compression of the shock, Sensor 1 coordinates (which are always the same) were subtracted from Sensor 2 coordinates in order to obtain the vector of the shock itself. The module was calculated and then the natural length of the shock [4] was subtracted to this value. This value represents the shock compression in negative and the shock extension in positive.
- For the Sensor 3, only they coordinates was used, as in the reference system of the car that is vertical travel, which is the one experimented by the wheel. After adjusting with the car height and wheel radius, the wheel travel was obtained.

With the values obtained it was possible to plot the installation ratio through all the wheel travel. This improved the reliability of the design and allow to slightly

modify the geometry of the Rear Bellcrank in order to obtain a constant installation ratio through wheel travel. Figure 5.25 shows the IR vs wheel travel. There is a discontinuity when the wheel travel is zero, as something divided by zero is infinite.

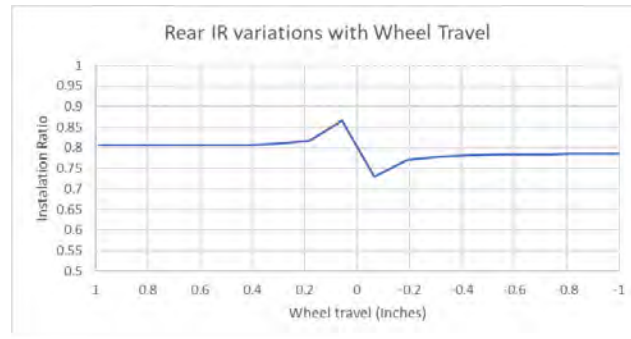


Figure 5.25: Rear Installation Ratio variation with wheel travel

### 5.10.3 Design space

The determination of the front bellcrank design space was even more complex because all the team assumed that the bellcranks were going to be placed in the same places as they were last year (Figure 5.26). One of the students tried to fit the front anti-roll bar in the last year's configuration and it was impossible to do without modifying other subsystems.

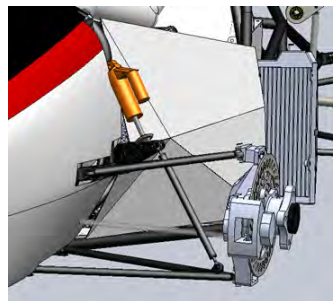


Figure 5.26: 2017 front bellcrank system

As the other subsystem will need to be modified, 3 different configurations were proposed:

- The first configuration or planar configuration was the best from the bellcrank point of view, but the worst for other subsystems. It was the best for the bellcranks as the push rod, the shocks and the wheel travel are all on the same plane. This caused that all the forces are always in the same plane, removing any bending moments in the bellcrank bearings and the installation ratio will be constant and easy to adjust because if all components are in the same plane the IR is the length of the shock lever arm to the pushrod lever arm. However, this configuration will cause the nosecone to be redesigned and required extra beams welded to the frame.

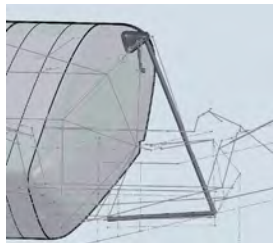


Figure 5.27: Planar configuration

- The second configuration proposed was a hybrid between the planar configuration and last years configuration. This configuration only required to cut part of the nosecone, but as it creates torsion in the frame, it was quickly discarded [10]. Figure 5.28 shows a picture of this type of bellcrank configuration.



Figure 5.28: Hybrid configuration

- The last configuration was an improvement of last years configuration. As all subsystem had designed with this in mind, the only modifications needed will be to cut a small aperture in the nosecone for the anti-roll bar, as shown in Figure 5.29. However, in this configuration, the installation ratio adjustment was not very intuitive and there was a high chance of it not being constant.

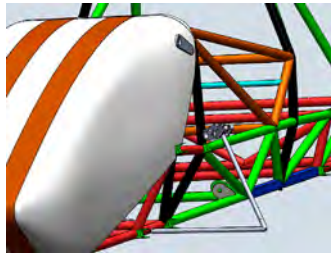


Figure 5.29: Improved Bellcrank configuration

After meeting with the advisor, the design lead, the body lead, and the suspension lead it was determined that the improved bellcrank configuration was the best option. There has been significant budget cut in this year car, as the team lost their main sponsor. The time constraint also discarded building a new nosecone. The only available option was to go with the improved configuration. After several iterations, Figure 5.22 depicts the front bellcrank design space. The front anti-roll

bar was placed on top of the frame as close as possible to the driver. This will minimize the amount of material cut from the nosecone.



Figure 5.30: Front bellcrank design space

The installation ratio plot of the front bellcrank is shown in figure 5.31. The limited space available forced to design a part that did not have a constant installation ratio. The clearance constraint is met during all the wheel travel.

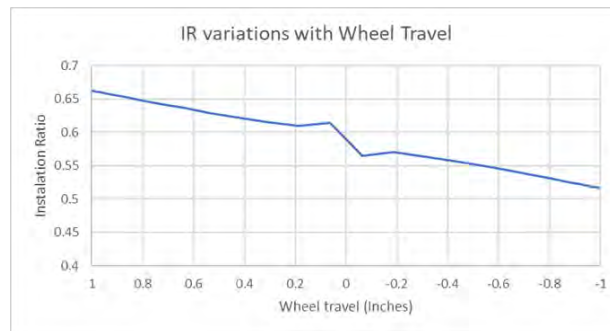


Figure 5.31: Front IR variation with wheel travel

#### 5.10.4 Topological optimization

A different approach was used regarding the topological optimization software. Instead of using the car reference system, the design space was made to have the origin and the planes matching the features of the part. This solution solved the

problem of the creation of a symmetry plane, but make it harder to calculate the force vector coordinates, as the DRS used a different origin. If the part reference system was going to be used in SolidThinking, this will imply to calculate all the force vectors by hand and to apply an orthogonal transformation or change of base to each one of them to match with the new base. While starting the process I realize that there was a better option; creating the part with the reference system in its center and then create an assembly in which the global reference system matched the part reference system. Then, introducing the Dynamic Reference Sketch and mate the front bellcrank sketch in the DRS to the actual bellcrank. This allowed me to obtain the coordinates of the force vectors in the base of the bellcrank. This method is slightly faster than the one used for the front bellcrank, but it is much simpler to understand for the undergraduate students.

The force calculations for the shocks were the same, however, for the ARB a different approach was used. A model of the ARB was created in SolidWorks and it was fixed in one end and constrained with a hinge fixture. This will force the bar to rotate only and not to bend. A model of the rocker plate was created too, applying the increasing force in the top of this part. By increasing the force, it is possible to discover which is the force that causes the FOS of the assembly to go under one. This force was 350 lbf instead of the 427 lbf obtained for the rear bellcrank as this time it was the rocker arm the part that failed first, so another FEA was run in the RBC to check and its FOS was 2.14. The FEA of the ARB can be seen in figure 5.32, when a force of 350 lbf is applied on top of the rocker plate. Is interesting to observe that it is the rocker plate and the union between the ARB and the rocker

plate the one failing.

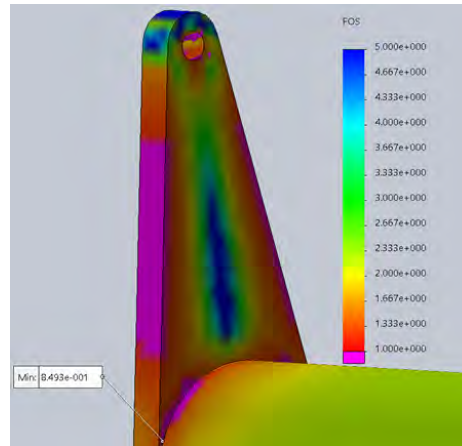


Figure 5.32: FOS plot for ARB

After calculating all the vectors, the symmetry plane was instantaneously added, and the FOS set to 2. The result is shown in Figure 5.33.



Figure 5.33: Front bellcrank topological optimization

Like in the RBC, a manufacturability analysis lead to a modification of the topological optimization design. As this time the topological optimization output was very coherent and in line with the load path no different configurations were tested. The final design was also split in two to facilitate the CNC machining and

can be seen in Figure 5.34. Again, extra material was added connecting the two fixtures. The manufacturing process is depicted in annex D.



Figure 5.34: Front bellcrank CNC model

#### 5.10.5 Front bellcrank final design

The definitive Front Bellcrank is shown in Figure 5.35

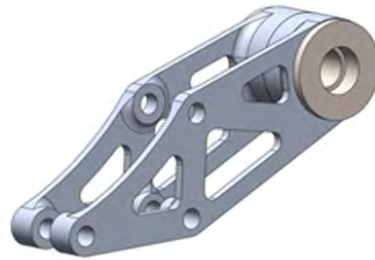


Figure 5.35: 2018 Front Bellcrank

The location of the front bellcrank system is depicted in figure5.36. The design specifications achieved are the followings:

- The Rear Bellcrank is 73% lighter.
- Has an average IR of 0.6 with a variation of  $\pm 7.5\%$  in max compression and extension.



- During max compression and extension, the maximum angle that forces make with the bellcrank plane is 4.3 degrees.
- It has built in spacers that make mounting easier.

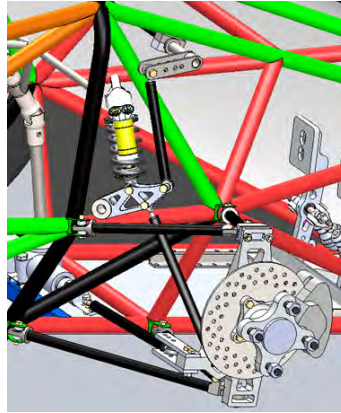


Figure 5.36: Front bellcrank system

## Chapter 6

## Project schedule and budget

Figure 6.1: Budget

Subsystem	Item	DEMAND	
		Monetary Budget	Non Monetary Budget
<b>Body</b>		<b>\$ (3,040.00)</b>	<b>\$ (2,825.00)</b>
	Steel Tubing	\$ (1,250.00)	
	Tube Cutting		\$ (1,500.00)
	Welding Jig Stock	\$ (100.00)	
	Frame Powdercoat		\$ (1,075.00)
	Mold Foam		\$ (50.00)
	Mold Machining		\$ (200.00)
	Fiberglass Fabric	\$ (200.00)	
	Mold Filler	\$ (200.00)	
	Layup Supplies	\$ (100.00)	
	Paint Primer	\$ (100.00)	
	Paint	\$ (100.00)	
	Harness	\$ (100.00)	
	Seat	\$ (85.00)	
	Steering Wheel	\$ (70.00)	
	Driver Attire	\$ (300.00)	
	Pedal Springs	\$ (60.00)	
	Pedal Potentiometers	\$ (100.00)	
	Pedal Assembly Stock	\$ (125.00)	
	Impact Attenuator	\$ (150.00)	
<b>Dynamics</b>		<b>\$ (9,970.00)</b>	<b>\$ (1,750.00)</b>
	Hardware	\$ (200.00)	
	Shocks	\$ (2,600.00)	
	Springs	\$ (70.00)	
	Steel Tubing	\$ (425.00)	
	Suspension Bearings	\$ (450.00)	
	Wheel Bearings		\$ (1,750.00)
	Upright Stock	\$ (575.00)	
	Wheel Hub Stock	\$ (200.00)	
	Wheels	\$ (1,000.00)	
	Wet Tires	\$ (800.00)	
	Dry Tires	\$ (1,800.00)	
	Brake Calipers	\$ (400.00)	
	Brake Master Cylinders	\$ (350.00)	
	Brake Tubing	\$ (150.00)	
	U-Joints	\$ (130.00)	
	Steering Rack	\$ (670.00)	
	Misc. Stock	\$ (150.00)	
<b>TOTAL</b>		<b>\$ (13,010.00)</b>	<b>\$ (4,575.00)</b>

ID	Task Mode	Task Name	Duration	Start	Finish
1		Introduction to frame team	7 days	Sun 9/3/17	Mon 9/11/17
2		Frame Rulebook	7 days	Tue 9/12/17	Wed 9/20/17
3		Frame Design documentation	7 days	Tue 9/12/17	Wed 9/20/17
4		FEA Beam Elements	3 days	Thu 9/21/17	Mon 9/25/17
5		Write base frame requirements	7 days	Thu 9/21/17	Fri 9/29/17
6		FEA model trouble shooting	14 days	Mon 10/2/17	Thu 10/19/17
7		Meshing original frame model	1 day	Fri 10/20/17	Fri 10/20/17
8		Torsional Stiffness research	7 days	Mon 10/23/17	Tue 10/31/17
3		Torsional Stiffness tests and mcl4 days	7 days	Wed 11/1/17	Mon 11/20/17
10		Torsional stiffness value for 2010 days	14 days	Mon 11/20/17	Mon 11/20/17
11		Design iterations for 2018 fram	14 days	Tue 11/21/17	Fri 12/8/17
12		Final frame design	0 days	Fri 12/8/17	Fri 12/8/17
13		Introduction to suspension test	7 days	Sun 12/10/17	Mon 12/18/17
14		Suspension Dynamics	14 days	Tue 12/19/17	Fri 1/5/18
15		Ride frequencies	7 days	Tue 12/19/17	Wed 12/27/17
16		Suspension Rulebook	7 days	Thu 12/28/17	Fri 1/5/18
17		Dynamic reference sketch	7 days	Mon 1/8/18	Tue 1/16/18
18		RBC Design Space	14 days	Wed 1/17/18	Mon 2/5/18
19		RBC Topological optimization	20 days	Tue 2/6/18	Mon 3/5/18
20		RBC design finished	0 days	Tue 2/6/18	Tue 2/6/18
21		FBC Design Space	10 days	Tue 3/6/18	Mon 3/19/18
22		FBC topological optimization	10 days	Tue 3/20/18	Mon 4/2/18
23		FBC design finished	0 days	Tue 4/3/18	Tue 4/3/18
24		Bellcranks manufacturing	14 days	Mon 4/23/18	Fri 4/20/18
25		Bellcranks manufactured	0 days	Mon 4/23/18	Mon 4/23/18
26		Excel tools and step by step guide	14 days	Mon 4/23/18	Thu 5/10/18

## Chapter 7

### Conclusions

#### 7.1 Frame

The 2018 frame was designed with three primary goals in mind. First, the frame needed to neatly package the accumulator, controls, and powertrain to maximize space efficiency in order to reduce the overall weight in the tubing. The accumulator's flatter design allowed it to protrude underneath the driver's seat. This created more room longitudinally which allowed for better packaging of the powertrain system. It also allowed simpler mounting of components above the accumulator. By having the frame contour the shape of the accumulator container, mounting for both the accumulator and the surrounding components required minimal additional tubing and shortened the moment arms of several mounts. The tubes surrounding the drivetrain were removed in order to reduce the weight and number of tubes required. This change necessitated closer packaging of the suspension and drivetrain but had the benefit of linking the front and rear suspension with fewer tubes and therefore creating a higher torsional rigidity.

Second, the cockpit was widened from the previous year to be accommodating to a wider variety of drivers. The front bulkhead was widened to support the standard impact attenuator and to create more leg room in the cockpit. The front roll hoop was also enlarged to create more space for the driver's knees. The driver

seat was reclined further as well in order to lower their center of gravity.

Finally, frame design was required to have a torsional rigidity of approximately ten times the suspension stiffness to provide proper structural support while cornering (approximately 2050 Nm/degree). Finite element analysis was used to determine the torsional rigidity before manufacturing. These simulations were used to make the frame as light as possible while maintaining the desired torsional rigidity. After multiple frame iterations, the simulation reported a torsional rigidity of 2114 Nm/degree.

The 2018 cockpit was designed to relieve the driver of physical stresses via mechanical advantage, comfort, and configurability. The general overarching design goals were chosen to accommodate drivers ranging in size from the 5th percentile female to the 95th percentile male. This required that an adequate amount of adjustability was implemented in order to maintain certain parameters. These parameters include a thigh angle of 15-19 degrees, a knee angle of 155-165 degrees, and proper spinal alignment with the head. These parameters required adjustability in pedal position and headrest depth while placing bounds on steering wheel location and seat orientation.

The 2018 pedal box is more robust, easier to adjust, and more adaptable. The force required to depress the accelerator was decreased to approximately 25 lbs to reduce driver fatigue during the race. Further, the new bias bar is centered about the pedal to make tuning the brake system both simple and accurate. Extensive FEA was performed on the pedal, frame mounts, and base plate to ensure that the pedal assembly can safely withstand the benchmark 2000N force, as well as to

optimize pocketing for increased weight reduction. Adjustability in pedal position was increased this year to 9 positions over a range of 9 inches. This allowed for all drivers to maintain proper leg geometry.

## 7.2 Suspension

The suspension design of the 2018 vehicle began by factoring in the driver skill, the desired driver comfort, and driver steering preference. This involved selecting appropriate ride frequencies, roll gradient, and understeer gradients. To begin, ride frequencies of 2 Hz and 2.5 Hz were selected as goals to bring the front and rear suspension back into phase after being perturbed by a bump. The characterization of the dampers damping rates was profiled for high speed and low-speed bumps. An estimation of the overall car weight distribution was then determined based off of iterations of the previous years car to determine the sprung mass resting on any given tire. Through iterative design, the desired motion ratio and spring rates were determined by taking into account the allowable shock travel, the spring rates that are commercially available, and desired amounts of vertical wheel travel. In the end, motion ratios of 0.6 and 0.8 and spring rates of 150 lbs/in and 200 lbs/in were chosen for the front and rear respectively. These were used to calculate front and rear suspension stiffnesses. From their, the desired roll gradient of 3 deg/lateral g was selected in order to provide the drivers with a sufficient amount of feedback. This roll gradient was used to calculate a total roll stiffness of the car (190 N-m/deg). The front-rear roll stiffness distribution of 55-45 was chosen to provide a desirable understeer gradient. This distribution and total stiffness were then used to design

anti-roll bars which would achieve those goals.

The control-arm design was centered around other aspects involved in driver comfort and vehicle performance include anti-dive, anti-squat, camber gain, and roll center migration. Anti-dive and anti-squat percentages were centered around 20% to reduce swaying. This value is derived from previous driver preferences. Camber gain and roll center migration were designed to be minimized through bumps and cornering. This was done by increasing the effective swing-arm length and by introducing unequal length control arms. These were constrained by packaging (driver and accumulator dimensions) and track length and iterated using Adams Car and in CAD. The caster and kingpin inclination were minimized in order to reduce driver fatigue in the endurance race. The construction of the control arms was altered this year to allow for simpler analysis and simpler manufacturability.

A pushrod suspension was selected this year to allow for a tighter packaging configuration. This resulted in more clearance for the bellcrank assembly. This years bellcranks benefited from a topological optimization overview that analyzed force distribution across the bellcranks geometry. The assembly was designed in order to achieve a relatively constant motion ratio and purely planar forces. Simulating loads from the pushrods and reactionary forces from the shocks, springs, and anti-roll bars allowed for visualization of the stress paths through the bellcrank plates. The topological optimization allowed for the reduction of mass using concentrated material placement around the lines of highest stress and strategic pocketing. The bellcrank was then constructed in two halves which were cut on a CNC mill to match the generated profile as closely as possible.



Designing the ARB for this year required significant attention towards mounting and packaging while abiding by the parameters selected above. Original concepts for the rocker plate were unstable and aesthetically displeasing due to their unoptimized nature and inefficient distribution of stresses. Simplifying the geometry to a basic elliptical shape allowed for expedited manufacturing and analyses. The pillow blocks are two separate segments that clamp around the actual roll bar to provide variable amounts of clamping force. Adjustability in stiffness was implemented in the rocker plates in order to tune the understeer gradient easily at competition.

### **7.3 Manufacturability**

Most parts can be made in a single setup, on a manual machine, using standard tooling. This simplicity affords us the ability to manufacture most of our parts in-house with a moderately skilled workforce. While simplicity is a focus, we are not limited to it. For 2.5 or 3 dimensional parts such as cell holders and uprights, we can use one of our CNC mills. Furthermore, our waterjet helps us quickly make sheet metal parts in large quantities. TIG welding expands our capabilities as well. Assembly is accomplished using mostly  $\frac{1}{8}$  bolts and a few instances of metric hardware, allowing for simple attachment and serviceability of subsystems.

### **7.4 Future works**

#### **7.4.1 Frame**

For the 2019 frame, there are some design improvements that are mandatory:

- The frame needs to be built in parallel with the front and rear suspension.

The 2018 frame was the first subsystem to be designed and it only used the hardpoints from the suspension, instead of thinking about the complete subsystem. This caused packaging problems for the suspension forcing to worsen the handling in order to achieve clearance.

- The main design goal of the frame was in compliance with the rulebook and subsystem placement. For 2019 frame, torsional rigidity and weight need to be at the same importance.

If the budget increase for next year a carbon fiber monocoque might be developed. The strongest carbon fibers are ten times stronger than steel and eight times that of aluminum, being 5 and 1.5 lighter, respectively [9]. This also eases the mounting of each subsystem, as there is no need to place the components in nodes for structural integrity. There is a UT SAE team that is already using this technology, but they have a budget of \$80000.



Figure 7.1: Carbon fibre monocoque

### 7.4.2 Suspension

For the 2019 bellcrank system, there are some major requirements: 2019 bellcrank system needs to start being designed at the same time as the frame. This will allow the frame team to design proper clearance and support for each element, without compromising the handling. It is mandatory to increase the budget and improve project management in order to be able to create prototypes. This will allow verifying the topological optimization accuracy. If budget increase, SLM manufacturing could be an option. Selective laser melting is a manufacturing technique which consists of melting aluminum powder using high energy lasers [5]. This allows manufacturing basically any geometry, which synergizes perfectly with the unusual geometries created by topological optimization. Figure 7.2 depicts the SLM process.

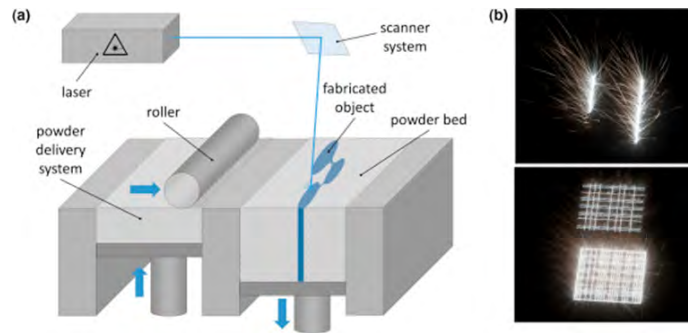


Figure 7.2: SLM process

Multi-body dynamics: Instead of using worst-case load for static simulations and then add a safety factor to account for the dynamic forces, the team should use multi-body dynamics. This approach consists in designing and model both right and left suspension in the software and then simulate a bump in the road [2]. Altair HyperWorks has all these capabilities plus topological optimization capabilities which

allow designing the parts in only one software without compatibility problems. It also accounts for the interaction between suspension

## Appendices

## Appendix A

### Calculations and selection of frame design modifications

The calculations performed in order to select the best design modification for the frame are depicted in this appendix. There are a total of 4 major test performed. Each test has a some design modification, that are going to be explained in each section. The values used to select the best design modification were primarily the torsional stiffness value, weight reduction and triangulation of the structure. The calculations performed to measure the torsional stiffness value were the same in all the test. A static analysis in SolidWorks, including the refined model obtained in section / and using a force value of 1500 lbf.

1. The frame model is fixed in the rear box by applying a fix geometry fixture in the four vertex that conform this box. Then, opposing forces of 1500 lbf were applied perpendicularly to the ground in the suspension model, in order to create a torque.
2. The simulation was run, and the displacement plot was set to display the y displacement, which is the one perpendicular to the ground.
3. The distance from the place where the force was applied to the neutral axis of rotation is measured. Using this value as hypotenuse and the y displacement as opposing leg, the angle of rotation is obtained.

4. The torsional stiffness is obtained as the torque, which is force times lever arm measured in step 3, divided by the angle twisted.
5. Finally, all the values are compared to the original model and percentages are given to facilitate judgment.

### A.1 Test 1

The first test is based in beam location. Different beams were tried in order to achieve full triangulation of the lateral panel and also an alternative front configuration based on the frame of the combustion team. A total of 5 modifications were tested:

- Modification 1.1: A triangulation of the lateral part of the frame by connecting the firewall mount to the front roll hoop as depicted in figure A.1

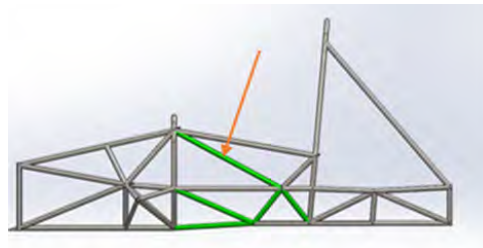


Figure A.1: Modification 1.1

- Modification 1.2: A combination between the modification 1.1 and the front top section of the internal combustion team. Figure A.2 depicts a top view of the internal combustion team frame. Two beams forming a cross can be seen in the front part of the car. That was the configuration tested, substituting

the horizontal bar that the original frame has:

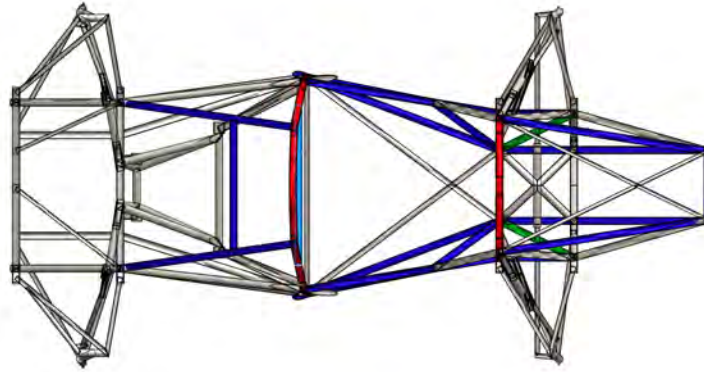


Figure A.2: Front top section of the internal combustion team

- Modification 1.3: This modification combined the internal combustion team front part of the frame with the beam configuration depicted in figure A.3

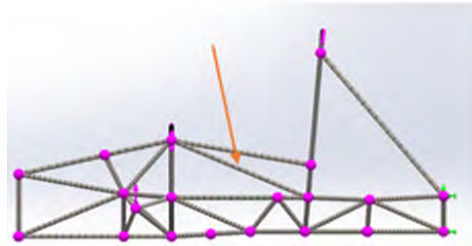


Figure A.3: Alternative lateral configuration

- Modification 1.4: In this modification only the alternative lateral configuration was tested.
- Modification 1.5: The final modification was the combination of the internal



combustion team front part with the original frame design of the team.

Table A.1 includes the most important values of all the parameters obtained during the test 1. Modification 1.1 was selected because it increased the k to a value close to the desired one and also provided a support for the firewall.

Table A.1: Test 1 results

Test 1	Force(lbf)	Y disp(mm)	angle(deg)	k (Nm/deg)
<b>Original conf.</b>	1500	12.32	1.16	1579.20
<b>Modification 1.1</b>	1500	9.62	0.90	2022.90
<b>Modification 1.2</b>	1500	7.79	0.73	2497.95
<b>Modification 1.3</b>	1500	8.45	0.79	2303.09
<b>Modification 1.4</b>	1500	10.22	0.96	1903.74
<b>Modification 1.5</b>	1500	10.49	0.99	1854.73
Test 1	FOS	Weight(lb)	% K	% lb
<b>Original conf.</b>	1.5	74.85	0.00%	0.00%
<b>Modification 1.1</b>	1.683	79.53	28.06%	6.25%
<b>Modification 1.2</b>	1.9	80.95	58.13%	8.15%
<b>Modification 1.3</b>	1.9	80.52	45.80%	7.58%
<b>Modification 1.4</b>	1.677	79.09	20.52%	5.66%
<b>Modification 1.5</b>	1.822	77.04	17.41%	2.93%

## A.2 Test 2

The second test focused on trying different tube thicknesses for the selected configuration in Test 1.

- Modification 2.1: The extra tube added has a thickness of 0.065 inches.
- Modification 2.2: The thickness was modified to 0.049.
- Modification 2.3: The thickness was modified to 0.035.

- Modification 2.4: The thickness was modified to 0.049 and the firewall support to 0.035.

The results are displayed in table A.2. The modification selected was the 2.4 as it provided a high k with a relative low increase in weight.

Table A.2: Test 2 results

Test 2	Force(lbf)	Y disp(mm)	angle(deg)	k (Nm/deg)
<b>Original conf.</b>	1500	12.32	1.16	1579.20
<b>Modification 2.1</b>	1500	9.62	0.90	2022.90
<b>Modification 2.2</b>	1500	9.90	0.93	1965.48
<b>Modification 2.3</b>	1500	10.28	0.97	1892.62
<b>Modification 2.4</b>	1500	9.92	0.93	1961.71
Test 2	FOS	Weight(lb)	% K	% lb
<b>Original conf.</b>	1.50	74.85	0.00%	0.00%
<b>Modification 2.1</b>	1.68	79.53	28.06%	6.25%
<b>Modification 2.2</b>	1.69	77.88	24.42%	4.05%
<b>Modification 2.3</b>	1.69	76.39	19.81%	2.06%
<b>Modification 2.4</b>	1.68	77.66	24.19%	3.75%

### A.3 Test 3

The modification in this section are focused in the triangulation of the front part of the frame, as the solution offered by the internal combustion team was proven inefficient in the test 1.

- Modification 3.1: This modification is actually a copy of the original design with the extra beam of 0.065 of wall thickness and 1 inch in diameter and is used as a second reference.
- Modification 3.2: This triangulation is depicted in figure A.4. The beam added

has 1 inch in diameter and a wall thickness of 0.035

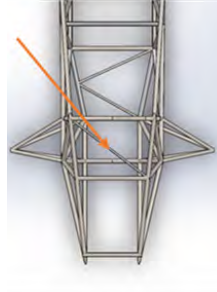


Figure A.4: Modification 3.2

- Modification 3.3: The same configuration as 3.2 but with a diameter of 0.75 and a wall thickness of 0.035
- Modification 3.4: The same configuration as 3.2 but with a diameter of 0.5 and a wall thickness of 0.028
- Modification 3.5: Triangulation of both top and bottom sections of the top front part of the frame. The modification can be seen in figure A.5

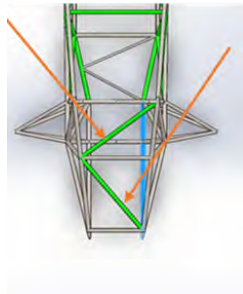


Figure A.5: Modification 3.4

The results of the test are displayed in table A.3. The modification chosen

was the 3.4, as the addition of an extra bar did not increase the k enough for the increase in weight.

Table A.3: Test 3 results

<b>Test 3</b>	<b>Force(lbf)</b>	<b>Y disp(mm)</b>	<b>angle(deg)</b>	<b>k(Nm/deg)</b>
<b>Original conf.</b>	1500	12.32	1.16	1579.20
<b>Modification 3.1</b>	1500	9.62	0.90	2022.90
<b>Modification 3.2</b>	1500	8.40	0.79	2316.80
<b>Modification 3.3</b>	1500	8.43	0.79	2307.18
<b>Modification 3.4</b>	1500	8.51	0.80	2285.77
<b>Modification 3.5</b>	1500	8.44	0.79	2304.45
<b>Test 3</b>	<b>FOS</b>	<b>Weight(lb)</b>	<b>% k</b>	<b>% lb</b>
<b>Original conf.</b>	1.50	74.85	0.00%	0.00%
<b>Modification 3.1</b>	1.68	79.53	28.06%	6.25%
<b>Modification 3.2</b>	1.87	80.24	46.67%	7.20%
<b>Modification 3.3</b>	1.83	80.05	46.06%	6.95%
<b>Modification 3.4</b>	1.81	79.80	44.70%	6.61%
<b>Modification 3.5</b>	1.89	80.08	45.88%	6.99%

#### A.4 Test 4

This is the last test performed and it was a combination of all the best results from the previous ones.

- Modification 4.1: This consisted in the original design of the frame with the modification 1.1 combined with the modification 3.4.
- Modification 4.2: This is a modification of 3.3 plus 3.4.

The results of the test are depicted in table A.4. The modification 4.2 was the definitive frame design for the 2018 car.

Table A.4: Test 4 results

<b>Test 4</b>	<b>Force (lbf)</b>	<b>Y disp(mm)</b>	<b>angle(deg)</b>	<b>k(Nm/deg)</b>
<b>Original conf.</b>	1500	12.32	1.16	1579.20
<b>Modification 4.1</b>	1500	8.83	0.83	2204.69
<b>Modification 4.2</b>	1500	9.20	0.87	2114.13
<b>Test 4</b>	<b>FOS</b>	<b>Weight(lb)</b>	<b>% k</b>	<b>% lb</b>
<b>Original conf.</b>	1.50	74.85	0.00%	0.00%
<b>Modification 4.1</b>	1.80	77.93	39.57%	4.11%
<b>Modification 4.2</b>	1.78	76.66	33.84%	2.42%

## Appendix B

### Rotation of SolidThinking Inspire Planes

The objective was to obtain the order and the degrees of rotation that each plane need to rotate in order to match with the part features, allowing the creation of a symmetry plain. FigureB.1 depicts the initial position of the planes:

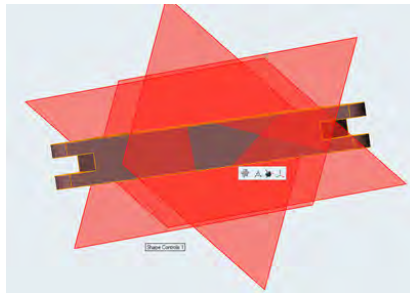


Figure B.1: Original orientation of Solidthinking planes

Using SolidWorks, a reference system bonded to the Bell Crank was created. Using 3D sketches perpendicular to the part faces and a center point to be the same as the one automatically created by Inspire, the body reference system was created in SolidWorks (Figure B.2).

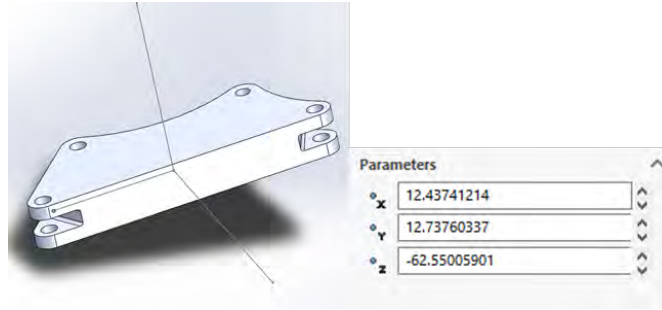


Figure B.2: SolidWorks reference system and point parameters tools

Then, the vectors of each 3D sketch were obtained, as the coordinates of each point were given by the SolidWorks, applying Equation B.1. They were normalized and arranged, each vector in a row of a matrix to create the change of basis matrix as in Equation B.2.

$$\overline{AB} = \overline{OB} - \overline{OA} \quad (\text{B.1})$$

$$E = \begin{pmatrix} e_{11} & e_{12} & e_{13} \\ e_{21} & e_{22} & e_{23} \\ e_{31} & e_{32} & e_{33} \end{pmatrix} \quad (\text{B.2})$$

Once the normalized base of the object was obtained, the inverse problem of Euler angles was solved, looking for the three Euler angles.  $\theta$ ,  $\psi$ , and  $\varphi$  are the 3 Euler's angle that describes the rotation, nutation, and precession of a solid. The first of Euler's angles were obtained using Equation 12. The nodal line is the normal line of the plane created by the  $k$  vector of the ground reference system and the  $e_3$  vector of the solid's base. It is the same vector as the ground's  $i$  vector after rotating the base the precession angle ( $i_1$ ).

$$\vec{e}_3 \cdot \vec{k} = e_{33} = \cos\theta \quad (\text{B.3})$$

$$\vec{e}_n = \vec{i}_1 = \frac{\vec{k} \times \vec{e}_3}{\sin\theta} \quad (\text{B.4})$$

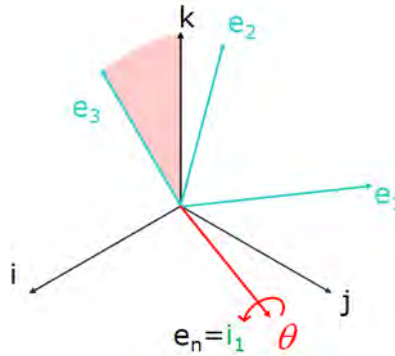


Figure B.3: Nodal line, nutation angle, ground reference system and body's reference system

The precession angle is the angle rotated from the ground's I vector to the nodal line or  $i_1$  vector. It is obtained with Equation B.5, as all vectors are normalized so their modulus is 1.

$$\vec{e}_n \cdot \vec{i} = e_{33} = \cos\phi \quad (\text{B.5})$$



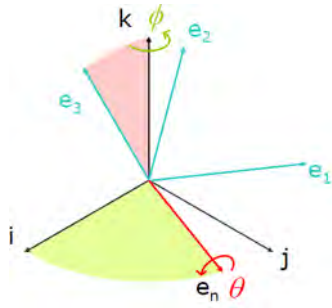


Figure B.4: Precession, nutation, and reference systems

The spin angle is the angle between the nodal line and  $e_1$  about  $e_3$ . As the nodal line is perpendicular to  $e_3$  and  $e_1$  is perpendicular to  $e_3$  too, both vectors are in the same plane. The spin angle is obtained in Equation B.6.

$$\vec{e}_n \cdot \vec{e}_1 = e_{33} = \cos\psi \quad (\text{B.6})$$

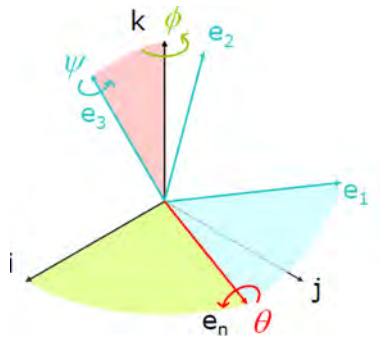


Figure B.5: Spin, nutation, precession, and reference systems.

Once the 3 Euler's angles are known, the ground reference system is rotated to make it align with the part reference system. Applying the rotations in order; precession, nutation, and spin in k, i and k respectively as depicted in Figure B.6.

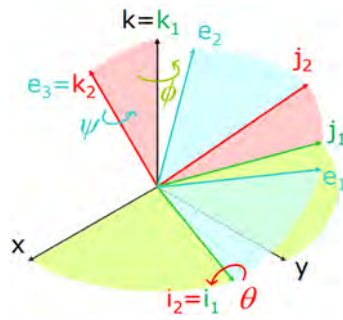


Figure B.6: Euler's angle rotation to align reference systems

The result of this process is shown in Figure B.7. Now it is possible to use the planes as symmetry plane for the topological optimization.

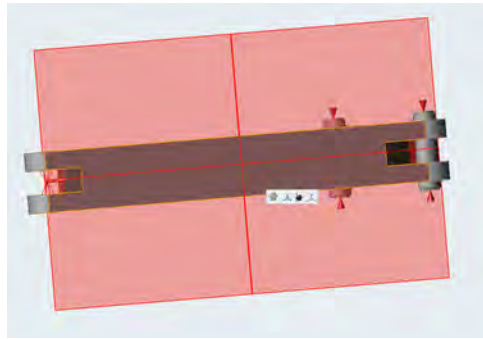


Figure B.7: Solid Thinking planes after applying Euler's rotation

## Appendix C

### Bellcrank system design guide

This guide is aimed to help the student to create an efficient bellcrank system. The guide assumes that the user has access to SolidWorks, has intermediate knowledge of the program, medium-high computational power and knowledge of suspension systems and terms. Finite Element Analysis knowledge and a license for Solid Thinking Inspire is required too. This guide is based on Long Horn Racing Electric Dynamic Reference Sketch created by Alex Choi.

#### C.1 Overview

The process of designing a bellcrank system starts with the determination of the Installation Ratios (IR). "Suspension System Design 01Dec2016" by Ronald Matthews can be used to calculate the IR, as is specified in the subsection 3 "The Ride Frequency Design Target". Then, an Assembly will be created in SolidWorks including all the components that interact with the bellcrank system. Properly creating mates will allow to create motion studies, that can incorporate a sensor feature to measure the IR. Then design iterations can be performed in order to achieve a the desired IR while also maintaining clearance. The maximum volume that the bellcrank can have will be obtained and introduced in the Topological optimization software, with the appropriate forces and fixtures. A factor of safety

will be chosen and then the program will generate an optimized geometry, that needs to be refined for 3-axis CNC machine.

## C.2 Step by Step guide

1. Calculation of Installation Ratios as explained in "Suspension System Design 01Dec2016" by Ronald Matthews.
2. Create a SolidWorks assembly including the Dynamic Reference Sketch (match with the origin of the assembly), the frame and other parts that might cause clearance problems, such as the nosecone and steering rack for the front suspension or the half shaft for the rear suspension. In case that parts are not finished or are too complex for your computational power, simplified models can be created. Sometimes is easier to create simple models using the Dynamic Reference Sketch than using existent ones, as they are normally very complex or parts of assemblies. Remember to define all dimensions if models are created.
3. Mate each part as accurate as possible, checking that the movement in the assembly make sense. 3D sketches representing the position of the A arm in maximum compression and tension need to be created to check that the assembly movement is the same as the one defined by the equations of the Dynamic Reference Sketch.
4. Once the clearance model is crated and moving as it is supposed, it is time to chose a location for the bellcrank, shock and push/pull rod. This are some

constraints that need to be achieved, if clearance allow it. Remember that you have the freedom to change from push rod suspension to pullrod suspension if it allow to accomplish more constraints:

- Clearance: The system must not interfere with any existing suspension member during the  $\pm 1.5$  inch wheel travel.
  - Bellcrank mount and shock mount to the frame must be in a node in order to avoid bending moments or torsion.
  - Planarity: The pushrod and the shock should be in the same plane as the bellcrank during wheel travel. The ARB needs to be placed where its forces remain in plane as much as possible. This avoids bending moments on the bellcranks bearing. As this is normally not possible, if the bellcrank has planar bearings, one of the components can be off plane. In my case, I chose the pushrod to be  $\pm 7$  degrees out of plane and the ARB to be  $\pm 5$  degrees. If packaging allows it, include the wheel travel in the bellcrank plane. This will make the IR adjustment infinitely easier.
5. Once the position of the system has been eyeballed, models of the pushrod and bellcrank need to be crated. First create a 3D sketch in the clearance assembly called "bellcrank system". This sketch will work as a model of the bellcrank system, where it is possible to play with the dimensions of the each sketch once it has been properly defined. It will have a shock mount consisting in a small line from the selected node (This will help to have the shock on plane

with the bellcrank) where the shock will be placed, defined by its length and 2 angles, the bellcrank mount the same as the shock mount, the bellcrank sketch defined with dimension between mounts and height to a neutral line and the pushrod reference by its length.

6. Now that the base dimensions have been defined in the sketch, actual models of each part should be created. It is not recommended to link the dimensions of the sketches to the parts as it will create problems during the motion study. Copy the dimension from the 3D sketch to the parts and then mate the parts to create accurate movement.
7. Check that the parts do not interfere with any other part during the specified wheel travel.
8. Activate the add in called motion study and go to the "Motion Study 1" tab that appear in the bottom of SolidWorks and choose motion study in the tab where "animation" appears.
9. Create an oscillation motor attached to the frame that makes the lower A arm move to the desired positions of maximum and minimum compression. If everything is mated right, the whole assembly should move as it will do in reality. Sometimes it is needed to change the integrator type in motion study properties to GSTIFF if the movement is not working.
10. Once it moves as it is supposed to, a sensor must be created using the results and plot feature and selecting the linear displacement function. This sensor will measure the absolute distance between the shock mount in the frame and

the shock mount in the bellcrank and the vertical displacement of the pushrod mount in the A arm. The results of the study must be exported to excel where the IR can be calculated by subtracting the shock natural length to the absolute shock length obtained and divided by the vertical travel. This IR should be as constant as possible and as close to the desire value as possible.

11. if it is not close to the desired value, start again from point 5. It is possible to modify the position of the bellcrank, shock and relative positions of the bellcrank mounts. There is no specific movement of parts that caused the IR to modify in a certain way. Try to move a bellcrank mount and see if the IR increase or decrease and then act in consequence. To make it more constant try to maximize planarity.
12. The hardest part is done now. The dimensions and location of the bellcrank system components is defined. It is important to obtain the maximum volume that the bellcrank can have without interfering with any other part (maximum logical volume, not maximum absolute). This part is called the design space and should take in account mounting interference with each hinge joint.
13. Now export the design space to Solid Thinking Inspire as a Parasolid, because Inspire does not work with SolidWorks student edition.
14. To calculate the coordinates of the forces, the design space of the bellcrank must be included in an assembly in SolidWorks where the origin and planes match with the bellcranks mid plane. Then add the Dynamic Reference Sketch and mate its bellcrank sketch to the design space. This will allow to obtain

the pushrod and shock vectors for compression and tension in the bellcrank reference system by subtracting point coordinates.

15. Introduce the loading cases of max compression and tension in Solid Thinking, the fixtures, the symmetry plain and specify a FOS of 2. Run the program and see the magic happening.
16. Export the model to SolidWorks and refine it for manufacturing
17. Your bellcrank is done!



## Appendix D

### Bellcranks manufacturing

The bellcranks manufacturing process has the following steps:

1. Creation of the CNC box. This rectangular prism encapsulate each bellcrank halves while leaving  $1/8$  of an inch for clearance. 4 rectangular prisms are needed for the front bellcranks and 4 for the rear bellcranks.
2. A rectangular prism made of aluminum was found in the shop, being a leftover from another project. The prism was marked as shown in D.1 to represent each CNC boxes.

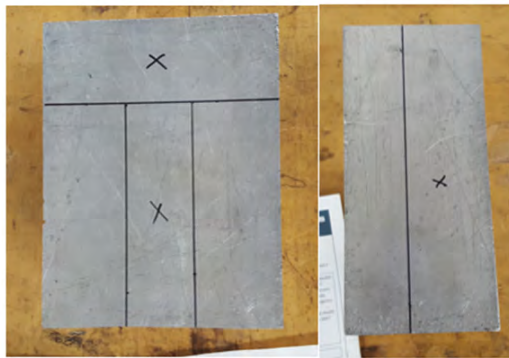


Figure D.1: Original aluminum prism

3. The aluminum prism was divided into smaller parts using the saw depicted in figure D.2. It was a semi automatic saw in which it was possible to set up a

cutting speed and the machine cut the part by itself while also refrigerating the part. A previous training was needed in order to use this type of machinery.



Figure D.2: Saw

4. As the saw was very old, the faces of the CNC boxes were not parallel. A facing machine was used in order to solve this problem as depicted in figure D.3



Figure D.3: Facing machine

5. The prepared CNC boxes are shown in figure D.4. It was important to create the boxes with the minimum material as possible as the CNC machine is used by all sub-systems, so minimizing the CNC time will improve the fabrication time of the car.



Figure D.4: CNC boxes

6. The final front bellcrank is depicted in figure D.5 and the final rear bellcrank

is depicted in D.6



Figure D.5: Final Front Bellcrank



Figure D.6: Final rear bellcrank

## Bibliography

- [1] Amy Chambers. *Development of a Test Stand for Determining the Torsional Rigidity of a Formula SAE Space Frame*. PhD thesis, The Cooper Union, 2016.
- [2] M Goelke. Practical aspects of multi-body simulation with hyperworks. *The HyperWorks University Team*, 2015.
- [3] SAE International. 2017-2018 formula SAE rules rev A.
- [4] SAE International. About formula SAE series.
- [5] K-H Leitz, P Singer, A Plankensteiner, B Tabernig, H Kestler, and LS Sigl. Multi-physical simulation of selective laser melting. *Metal Powder Report*, 72(5):331–338, 2017.
- [6] LongHorn Racing. What we do.
- [7] Carroll Smith. *Tune to win*. Aero publishers Fallbrook, 1978.
- [8] SolidWorks. Integration methods.
- [9] SolidWorks. Modeling an fsae frame - tutorial - solidworks.
- [10] Formula Student. Pats seven deadly sins of fs design.

## Index

- 4.3. Installation ratio calculation for 2018 bellcranks, 35*
- Abstract, vi*
- Acknowledgments, v*
- Anti-roll bar (ARB), 38*
- Appendices, 77*
- Appendix*
  - Bellcrank system design guide, 91, 97*
  - Calculations and selection of frame design modifications, 78*
  - Drawings, 104*
  - Rotation of SolidThinking Inspire Planes #2, 86*
- Background of need, 4*
- Bellcrank Design, 34*
- Bellcrank system, 34*
- Bibliography, 101*
- Chassis, 1, 14*
- Conclusions, 69*
- Customer information, 4*
- Customer Needs Statement, 5*
- Dedication, iv*
- Design methodology, 18, 40*
- Design modifications for 2018 frame, 30*
- Design objectives, 15, 39*
- Design Space, 43*
- Design space, 58*
- Dynamic Reference Sketch, 37*
- Final rear bellcrank design, 51*
- Frame, 10, 69, 73*
- Frame Design, 14*
- Front Bellcrank Design, 52*
- Front bellcrank final design, 64*
- Functional Requirements, 6*
- Future works, 73*
- Introduction, 1*
- Long Horn Racing Electric working methodology, 7*
- Manufacturability, 73*
- Motion study, 53*
- Motion study refinements, 54*
- Nosecone, 39*
- Preparation of 2018 model for FEA, 23*
- Previous work, 14, 35*
- Project schedule and budget, 67*
- Rear Bellcrank Design Process, 41*
- State of the art, 10*
- Suspension, 2, 11, 71, 75*
- Topological optimization, 45, 61*
- Torsional stiffness accuracy, 26*
- Torsional stiffness calculation for 2017 frame, 19*
- Torsional stiffness calculation for 2018 frame, 23*
- Vehicle requirements, 6*

## Vita

Francisco Javier Suarez was born in Santa Cruz de Tenerife, Spain on 23 March 1994, the son of Dr. M. Mercedes Suarez and Francisco J. Suarez. He received the Bachelor of Science degree in Electromechanical Engineering from the Pontifical University of Comillas. He applied to the University of Texas at Austin for enrollment in their civil engineering program. He was accepted and started graduate studies in August, 2017.

Permanent address: 2505 Longview street  
Austin, Texas 78705

This thesis was typeset with L<sup>A</sup>T<sub>E</sub>X<sup>†</sup> by the author.

---

<sup>†</sup>L<sup>A</sup>T<sub>E</sub>X is a document preparation system developed by Leslie Lamport as a special version of Donald Knuth's T<sub>E</sub>X Program.

## Appendix E

### Drawings



**LONGHORN RACING ELECTRIC  
UNIVERSITY OF TEXAS AT AUSTIN  
2018 VEHICLE**

**DETAILS:**

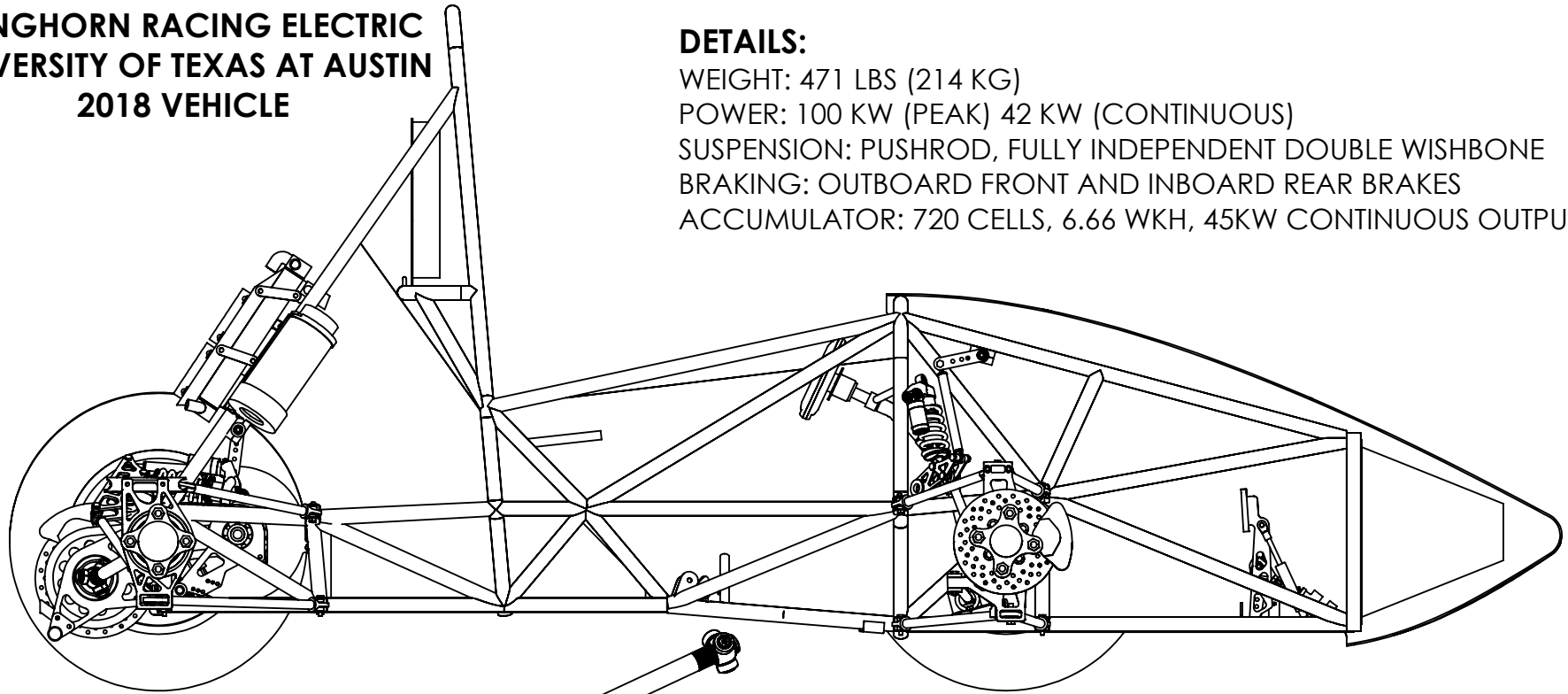
WEIGHT: 471 LBS (214 KG)

POWER: 100 KW (PEAK) 42 KW (CONTINUOUS)

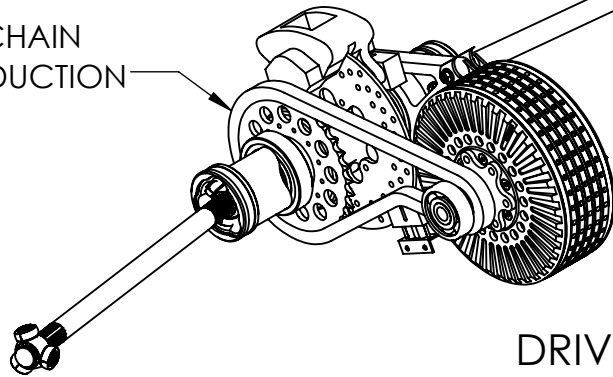
SUSPENSION: PUSHROD, FULLY INDEPENDENT DOUBLE WISHBONE

BRAKING: OUTBOARD FRONT AND INBOARD REAR BRAKES

ACCUMULATOR: 720 CELLS, 6.66 WKH, 45KW CONTINUOUS OUTPUT

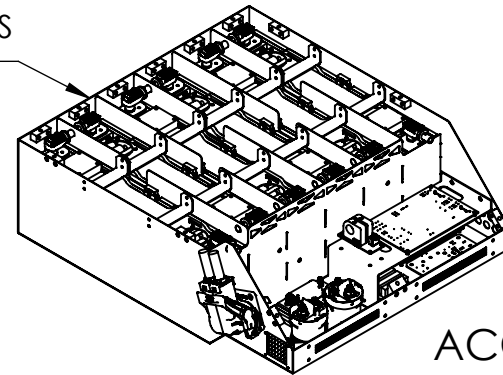


#520 CHAIN  
3:1 REDUCTION



**DRIVETRAIN**

720X 18650 CELLS  
3.7V 2500MAH



**ACCUMULATOR**



Configuration: Default

Printed on 4/2/2018 Sheet 1 of 3

**TOLERANCES (unless otherwise specified):**

- +/- .005 on flat pattern
- +/- .010 on bends
- +/- 1/2 deg angles
- +.003/- .001 on holes
- +/- .010 on Csink dia & thru hole

**PROPRIETARY AND CONFIDENTIAL**

**LHR Electric**

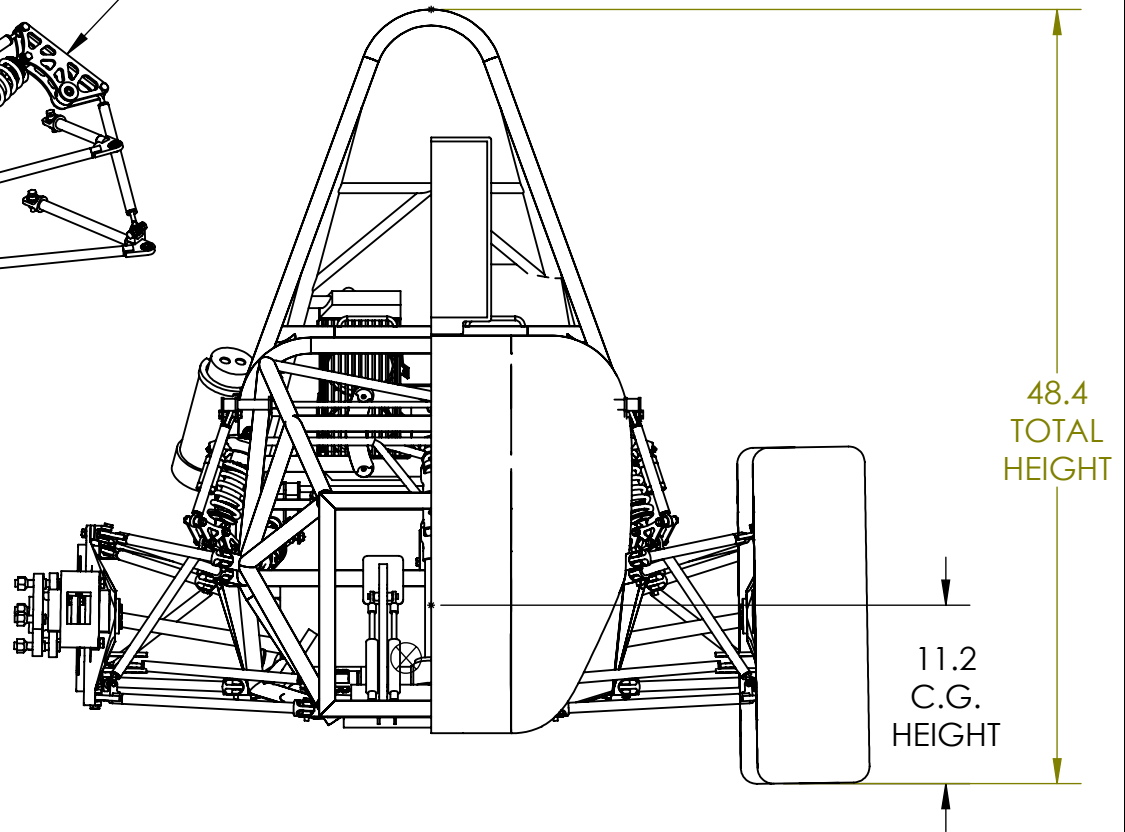
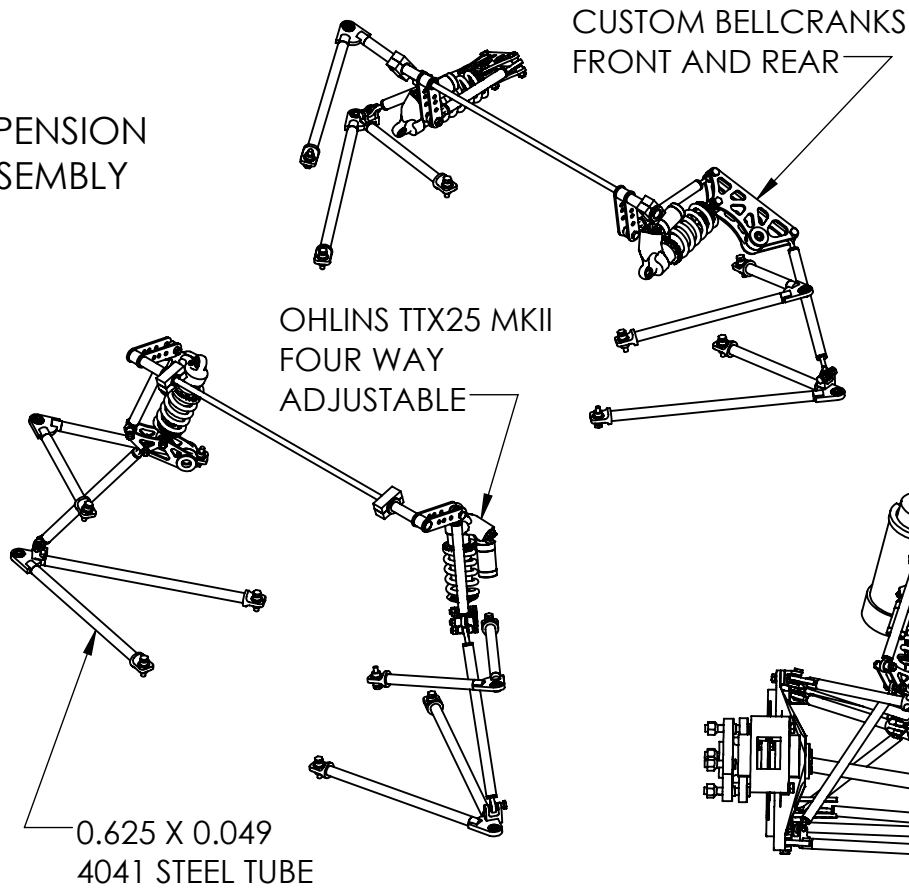
2018 LHRE FSAE ELECTRIC VEHICLE

Dwg No & Rev

18-000

**LONGHORN RACING ELECTRIC  
UNIVERSITY OF TEXAS AT AUSTIN  
2018 VEHICLE**

SUSPENSION  
ASSEMBLY



Configuration: Front View

Printed on 4/2/2018 Sheet 2 of 3



**TOLERANCES (unless otherwise specified):**

- +/- .005 on flat pattern
- +/- .010 on bends
- +/- 1/2 deg angles
- + .003/- .001 on holes
- +/- .010 on Csink dia & thru hole

**PROPRIETARY AND CONFIDENTIAL**

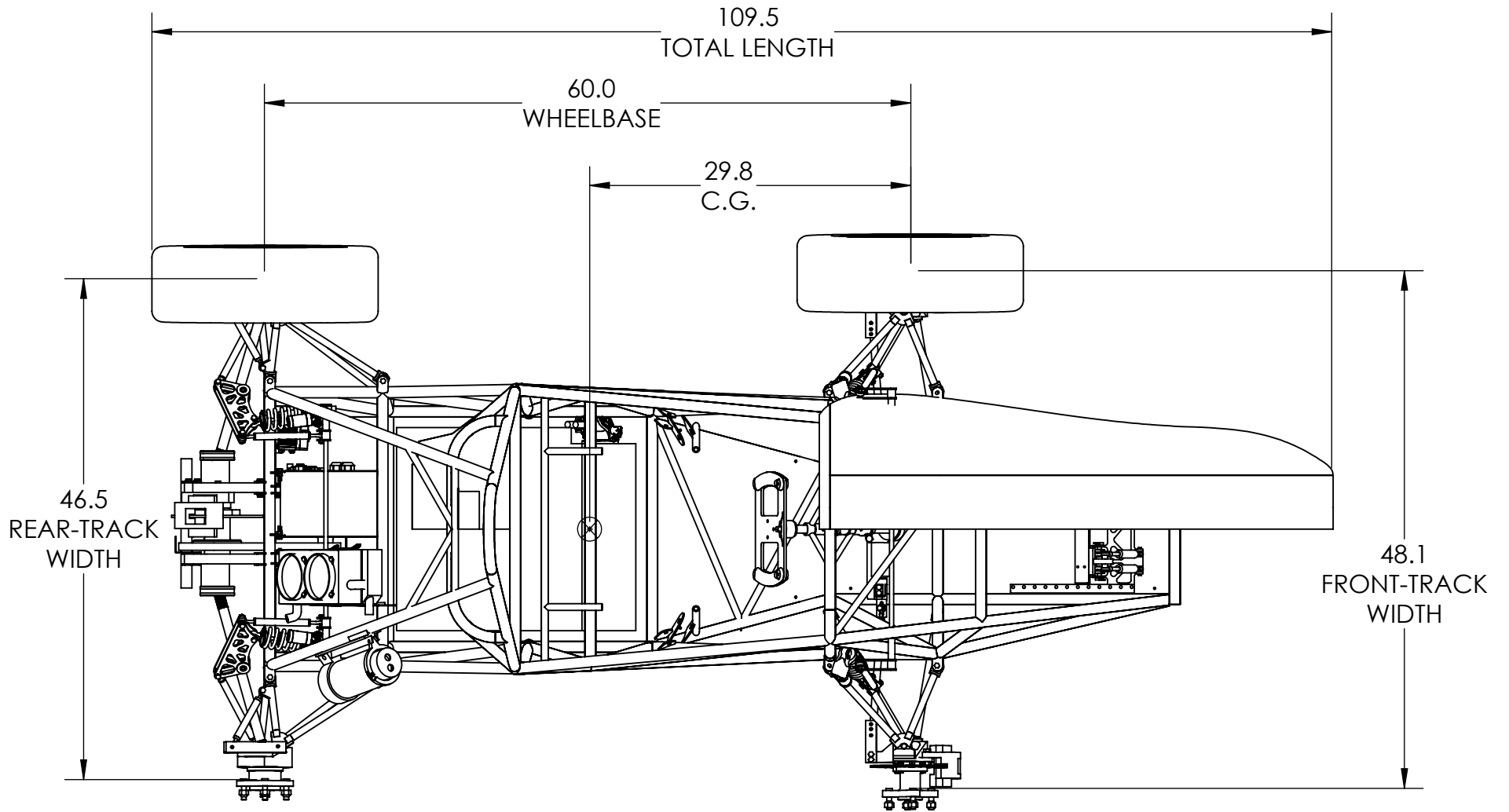
**LHR Electric**

ALL DIMENSIONS IN INCHES

Dwg No & Rev

18-000

# DIMENSIONS



Configuration: Front View

Printed on 4/2/2018 Sheet 3 of 3



**TOLERANCES (unless otherwise specified):**

- +/- .005 on flat pattern
- +/- .010 on bends
- +/- 1/2 deg angles
- +.003/- .001 on holes
- +/- .010 on Csink dia & thru hole

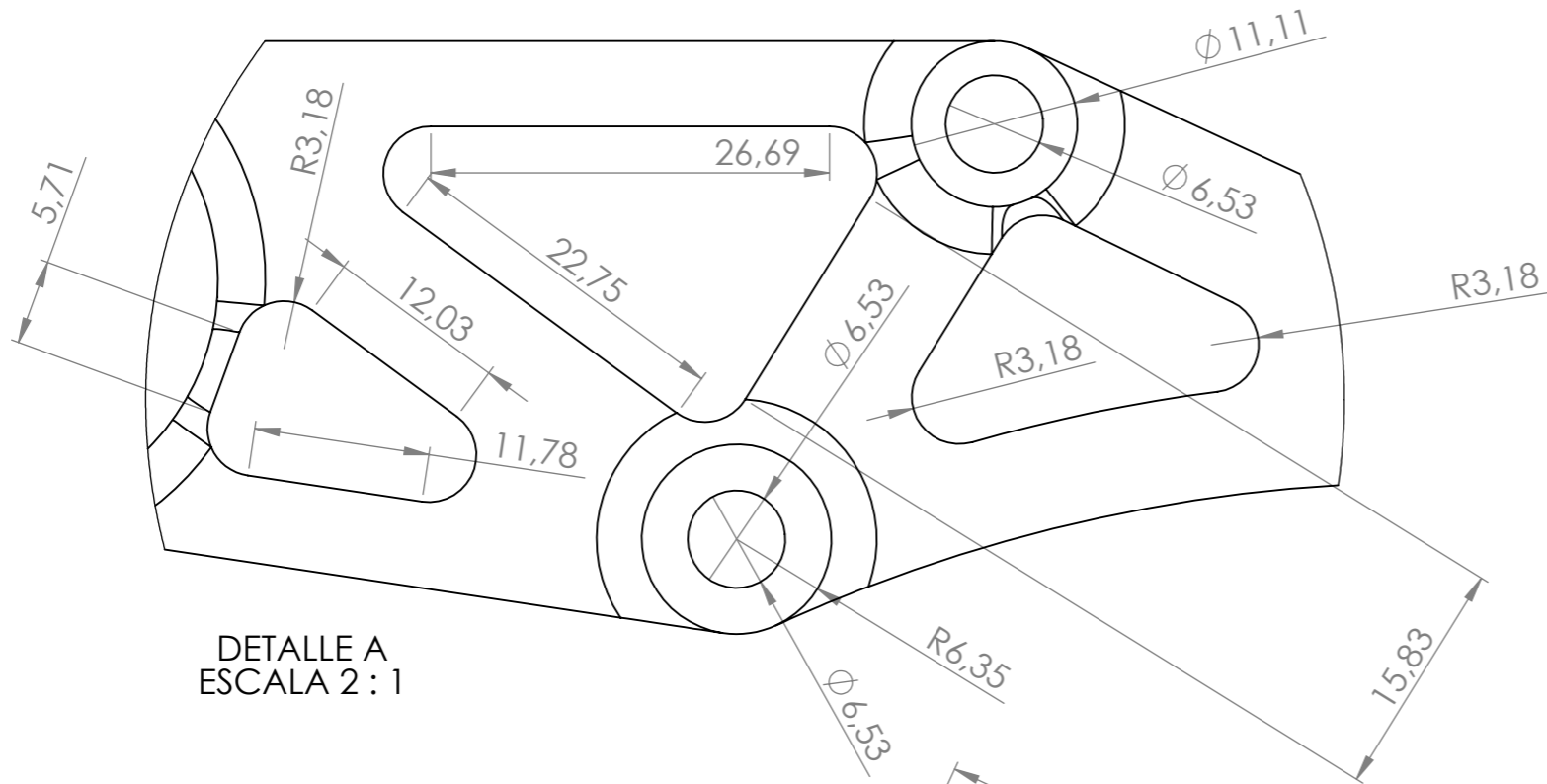
**PROPRIETARY AND CONFIDENTIAL**

**LHR Electric**

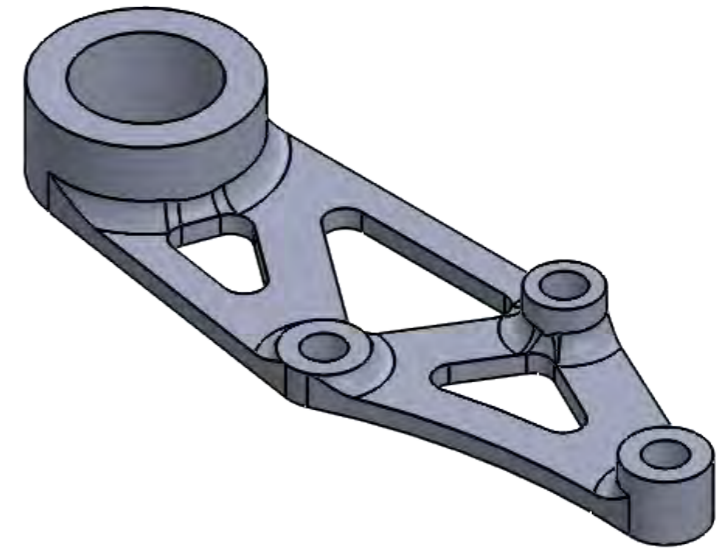
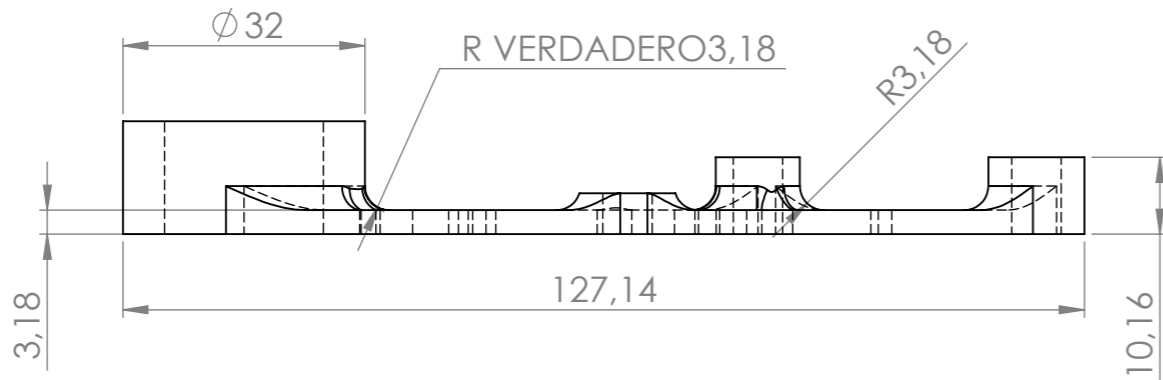
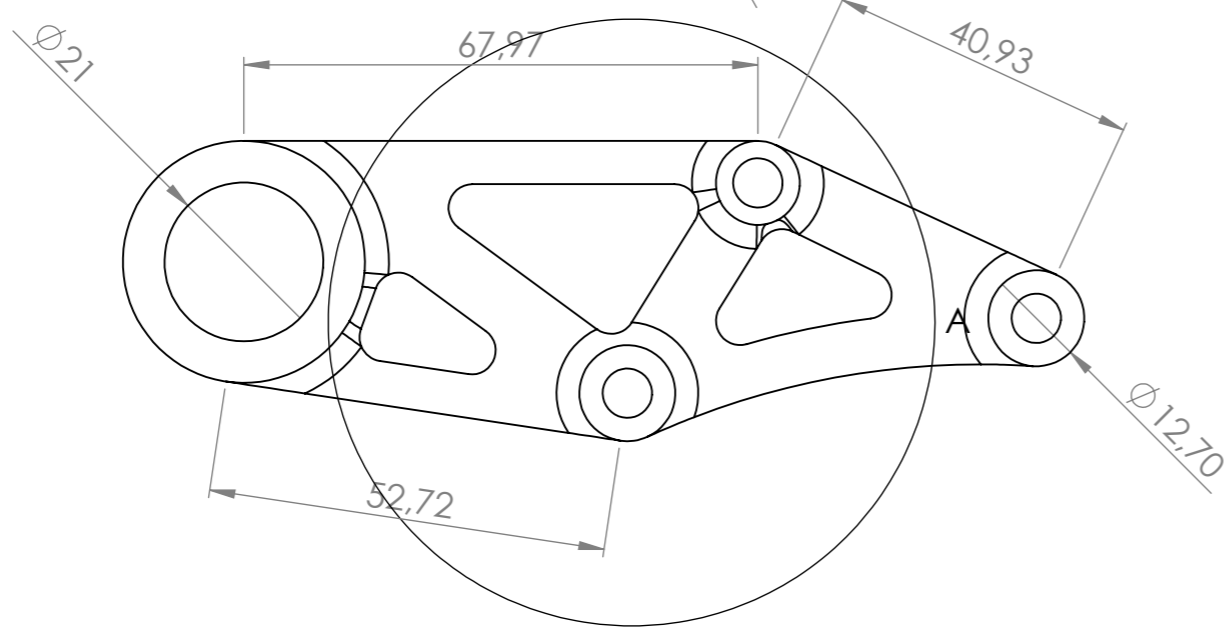
ALL DIMENSIONS IN INCHES

Dwg No & Rev

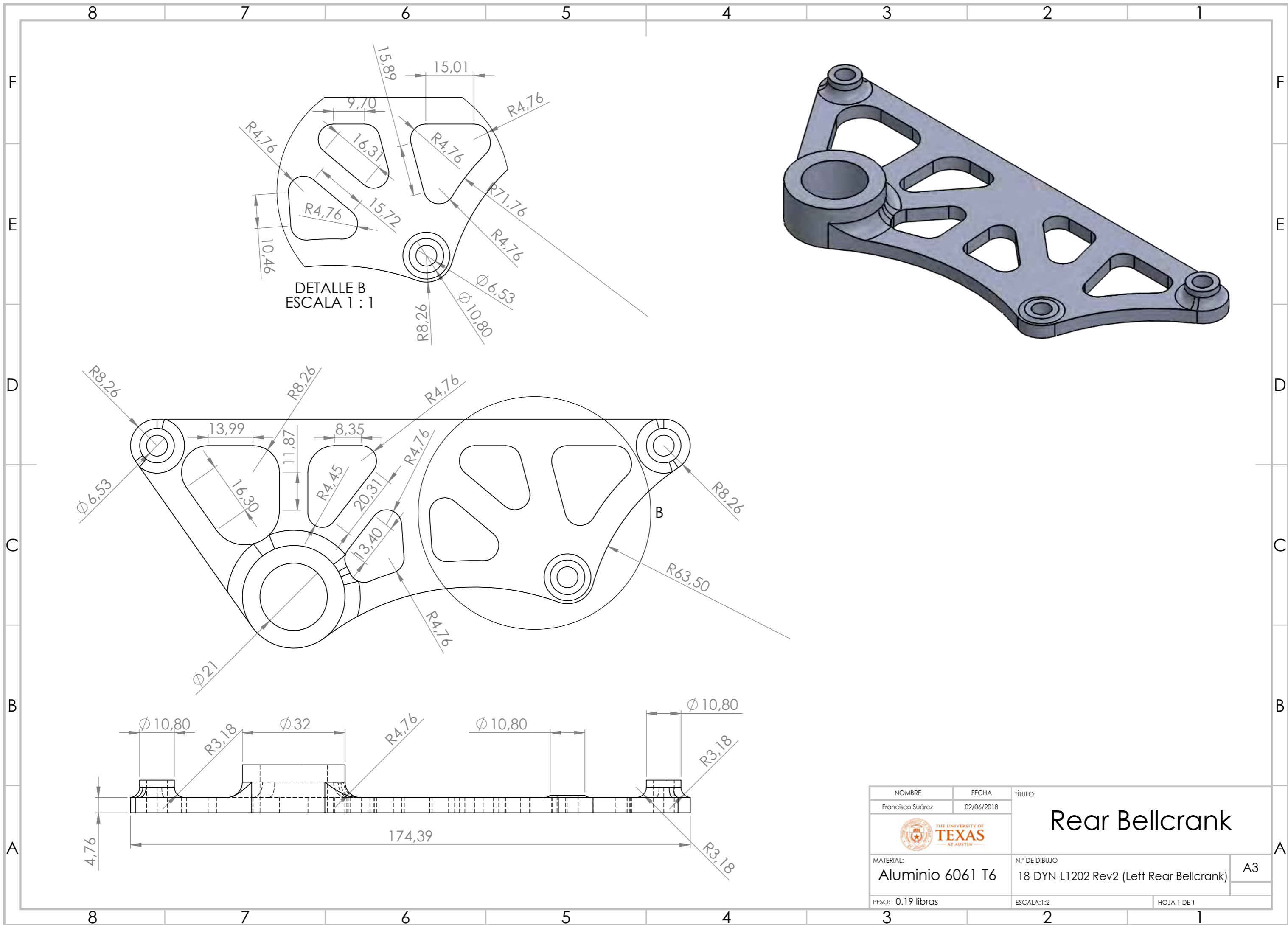
18-000



DETALLE A  
ESCALA 2 : 1

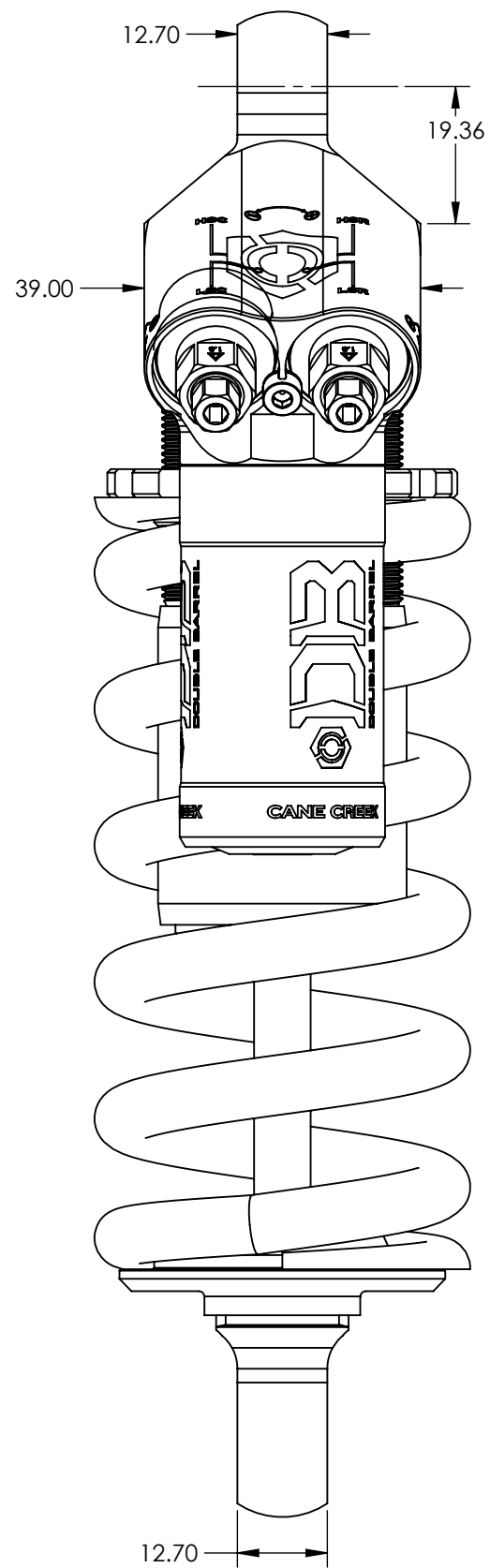
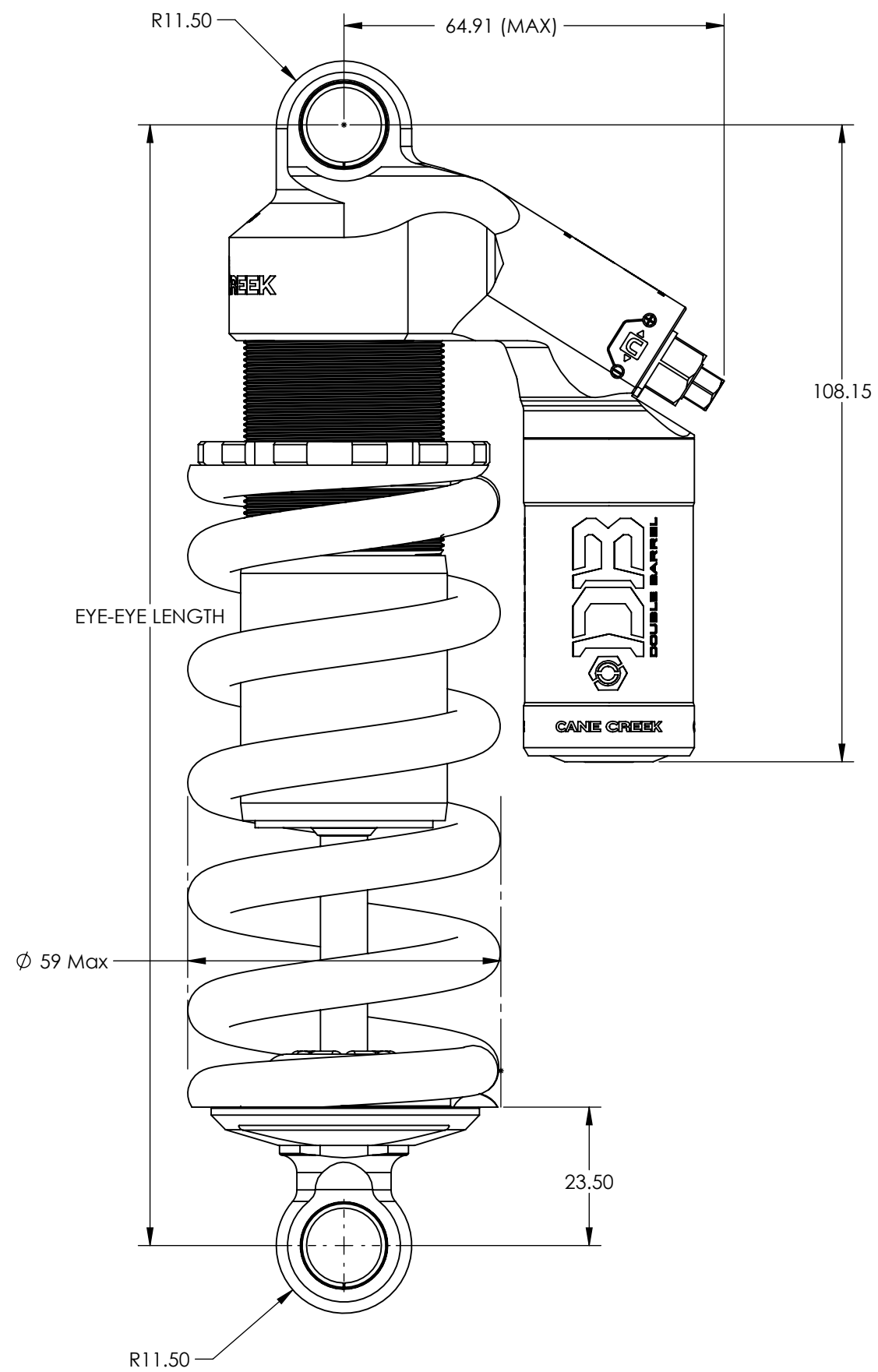


NOMBRE	FECHA	TÍTULO:
Francisco Suárez	02/06/2018	Front Bellcrank
		N.º DE DIBUJO
MATERIAL:		A3
Aluminio 6061 T6		18-DYN-L1201 Rev2 (Left Front Bellcrank)
PESO: 0.09 libras	ESCALA:1:1	HOJA 1 DE 1



NOMBRE	FECHA	TÍTULO:
Francisco Suárez	02/06/2018	<b>Rear Bellcrank</b>
		
MATERIAL:	N.º DE DIBUJO	A3
Aluminio 6061 T6	18-DYN-L1202 Rev2 (Left Rear Bellcrank)	
PESO: 0.19 libras	ESCALA:1:2	HOJA 1 DE 1





- Notes:
- 1.) Refer to owners's manual for Eye-Eye length and Travel
  - 2.) 64.91 mm Max with adjusters turned full clockwise
  - 3.)  $\phi$  59mm Max with largest coil

mm Dimensions		This drawing and all information therein is the property of Cane Creek Cycling Components and is confidential and must not be made public or copied. It is loaned subject to return upon demand and is not to be used in any way that is detrimental to our interests.			
Tolerances: .X $\pm$ 0.3 .XX $\pm$ 0.10 .XXX $\pm$ 0.05  Angular: $\pm$ 0.5 Concentricity: 0.10  Third Angle Projection					
Material:		SIZE	Part No.	REV.	
Weight:		B		01	
Finish: Bright Anodized		Color: Black/Gold		SCALE: 1:1	SHEET 1 OF 1